Digital Transmission in the Presence of Impulsive Noise*

By J. S. ENGEL

(Manuscript received April 4, 1965)

The transmission of digital data over telephone channels has been considered previously in the literature, and the effects of Gaussian noise have been analyzed. With experience, however, it has become apparent that while a background of Gaussian noise is present, the limiting noise is not Gaussian but impulsive in nature. It consists of bursts of high amplitude which occur at random considerably more often than is predicted by the rms value of the Gaussian background noise.

Measurements of the statistics of this noise have been initiated, and some results have been reported. In this paper, a model for the noise is constructed to be reasonably consistent with these measurements without becoming too complex to be handled analytically. Various modulation systems are analyzed to determine their performance in such a noise environment. Conditional error rates, in terms of the average number of bit errors per noise burst, are determined as functions of a convenient signal-to-noise ratio which is defined. The systems are ranked as to their performance in such a noise environment, and the ranking is found to be the same as that for Gaussian noise.

The improvement to be gained by employing complementary delay networks is investigated. Networks with linear and sinusoidal delay characteristics are considered.

I. INTRODUCTION

The limiting noise with regard to transmitting digital data is impulsive in nature. Consisting of bursts of high amplitude, it occurs at random considerably more often than is predicted by the rms value of the Gaussian background noise. In this paper, an analysis is made of digital transmission, by various modulation procedures, in such a noise environment.

* Taken from the dissertation submitted to the Faculty of the Polytechnic Institute of Brooklyn in partial fulfillment of the requirements for the degree of Doctor of Philosophy, 1964.

The block diagram of a generalized data transmission system including a telephone channel is shown in Fig. 1. The data signal consists of a train of either ideal impulses or square pulses, each pulse having either positive or negative polarity depending on whether it represents a mark or a space. The transmitter consists of a low-pass filter, which band limits the data signal, followed by a modulator and a band-pass filter. The low-pass filter is required to prevent "foldover" distortion in modulation. The band-pass filter restricts the transmitted signal to the range of frequencies passed by the channel. It avoids the waste of transmitted power in signal components which will not be received and also includes the channel splitting filters which prevent crosstalk into frequencies reserved for other channels. The low-pass and band-pass filters also shape the signal, giving it the form desired for transmission. The transmitted signal is applied to the channel, where it is contaminated by additive noise. The combined signal and noise enters a receiver which consists of a band-pass filter and demodulator which is generally followed by a low-pass filter and a synchronous decision device. The band-pass filter removes components of the noise outside the band of the signal, in addition to shaping the received signal. The low-pass filter, which is not required in every system, removes the demodulation products which lie outside the band of interest, and may also provide further signal shaping. The decision device samples the combined signal and noise at its input at discrete sampling instants, and on the basis of each sample, produces a mark or space symbol.

The channel is band limited, and may have an amplitude versus frequency characteristic which is not flat and a phase versus frequency characteristic which is not linear. However, for the purposes of analysis, the exact characteristics of the channel may be lumped with those of the receiver band-pass filter. The channel may then be considered as having the characteristics of an ideal band-pass filter, with unity gain and zero phase shift in the band of interest.

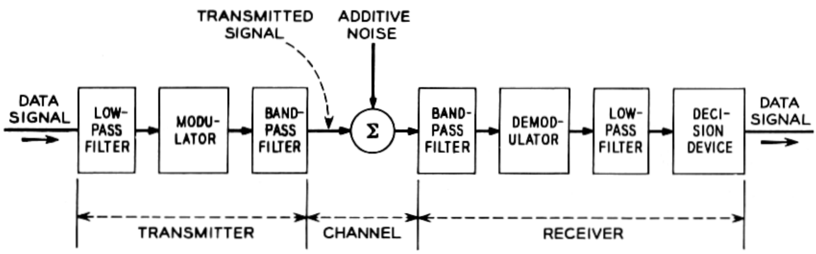

Fig. 1 — Generalized data transmission system.

The very broad objective, in considering such a problem, is to design the transmitter and receiver so that the number of errors caused by the noise is minimized, under the constraint that the average power of the transmitted signal is limited. A corollary objective, and obvious prerequisite, is to derive an expression for this error rate as a function of some readily measured signal-to-noise ratio, with the system characteristics as parameters. Then, one or two simple measurements of the noise on the channel will suffice to predict the error rate which can be expected of any system.

In this paper, various existing modulation systems are considered. The specific problem, then, is to find a suitable mathematical model for the noise, and for each system, to determine the response of the demodulation procedure to the combination of the signal and such noise. The processed noise at the output of the demodulator and filters is the source of the errors by the decision device. The optimization procedure consists of finding the decision criterion and filter characteristics at the receiver which minimize the number of errors caused by the noise, under the constraint of average power limiting of the transmitted signal. For each modulation system, this procedure specifies the receiver design, except for the phase characteristic of the receiving filter. In order to avoid intersymbol interference at the decision device, a specific functional form for the signal at that point is required. Given the filter characteristics at the receiver, as determined by the optimization procedure, the filter characteristics at the transmitter are made such that the response of the over-all transmission path to the applied data signal is the specific signal required at the decision device. This specifies the transmitter design for each modulation system.

In this paper, the following modulation systems are analyzed to determine their performance in the presence of impulsive noise:

(1.) Double sideband AM with coherent detection
(2.) Single sideband AM with coherent detection
(3.) AM with envelope detection
(4.) Frequency shift keying with frequency discrimination
(5.) Binary phase shift keying with differentially coherent detection
(6.) Quaternary phase shift keying with differentially coherent detection.

Conditional error rates, in terms of the average number of bit errors per noise burst, are determined as functions of a signal-to-noise ratio which is defined in the following section. The systems are ranked as to their performance, in order of increasing conditional error rate. This ranking is found to be the same as that for performance in the presence of Gaussian noise, and agrees with the ranking experienced in actual usage.

In the analyses, it is found that the phase characteristics of the receiving filter affect the performance of the system. This phenomenom, which is not present when the noise is Gaussian, leads to the consideration of complementary delay filters. Three types of delay filters are considered, and the improvement which results from their use is found, as a function of the maximum delay of the filter, for each of the modulation systems.

II. MODEL FOR THE IMPULSE NOISE

As previously described the various data transmission systems include modulation and demodulation of a carrier frequency. The data receivers each include a band-pass filter. For the purposes of analysis, the actual characteristics of the channel are lumped with those of the band-pass filter, and the channel is considered as having the characteristics of an ideal band-pass filter. With double-sideband transmission, these characteristics are made symmetrical about the carrier frequency. The impulse noise present on such a channel consists of bursts of carrier frequency ω_c, with random phase ψ, occurring randomly in time. When single-sideband transmission is used, the characteristics are asymmetrical and the Hilbert transform of the envelope is also present. This however, merely modifies the envelope and phase of the noise burst. The actual noise, as it occurs in the telephone plant, is wideband, with a spectrum covering many channels. The noise burst at the output of any one channel is the response of the channel to the wideband noise and contains only a small portion of the total spectrum. It is reasonable to assume therefore, that the spectrum of the noise burst at the output of the channel is essentially determined by the channel characteristics, with the original spectrum of the wideband noise having little effect. Under this assumption the envelope of each noise burst is the same, except for a random amplitude K. This is of course, an approximation. The spectra of the noise bursts do vary somewhat. However, in order to be useful, a model must be reasonably consistent with the observed phenomena without becoming too complex to be handled analytically. Approximating the envelopes of the noise burst by a representative time function $n_0(t)$ is a very reasonable approximation. At this point in the analysis, the envelope $n_0(t)$ is not limited to any particular function. A general expression for the error rate is derived, into which any specific function may be inserted. Then in order to obtain numerical results, a specific function is assumed. Up to that point, however, the analysis is quite general.

A single noise burst of carrier frequency $n(t)$, occurring at time $t = \tau$, may be represented in the form:

$$n(t) = Kn_0(t - \tau) \cos (\omega_c t + \psi) \tag{1}$$

where K, τ, and ψ are three independent random variables associated with each burst. For ease of notation, the envelope $n_0(t)$ is normalized to have an energy of two watt-seconds. Then, the energy ε of the noise burst $n(t)$ is equal to K^2.

Measurements have been made on representative telephone channels, to determine the statistical characteristics of the noise.[1,3] As a result, there have been functional forms for:

$$F(x) = Pr[K > x] \tag{2}$$

suggested by Fennick,[3] Mertz,[5,6] and others, which fit the measured data reasonably well for the range of K large enough to cause errors. These are families of functions $F_\alpha(x)$, where the parameter α may vary from channel to channel but is constant for any one channel. One such family of functions, suggested by Mertz, which fits the data reported on by Fennick, is computationally suited to this development. A reference amplitude K_0 is chosen sufficiently low in value that any noise burst which might cause an error would have an amplitude greater than K_0. The relative frequencies of amplitudes greater than K_0 are measured and plotted. That is to say, the conditional probability

$$\Pr[K > x \mid K > K_0]$$

is plotted versus the relative amplitude

$$20 \log_{10}(x/K_0) db.$$

These plots are straight lines on logarithmic paper, as shown in Fig. 2. The negative slope of each line, in decades per 10 db, is the parameter α. These plots satisfy the equation

$$\Pr[K > x \mid K > K_0] = (K_0/x)^{2\alpha}. \tag{3}$$

When describing the impulse noise, it is sufficient to consider only those bursts with amplitude greater than K_0; if K_0 is chosen low enough that bursts with smaller amplitude do not cause errors, these smaller bursts may be ignored and artificially assumed not to occur. Then, the family of functions F_α(a) is given by:

$$F_\alpha(x) = \Pr[K > x] = (K_0/x)^{2\alpha} \quad \text{for} \quad x > K_0. \tag{4}$$

The majority of the measured distributions have values of α between 1

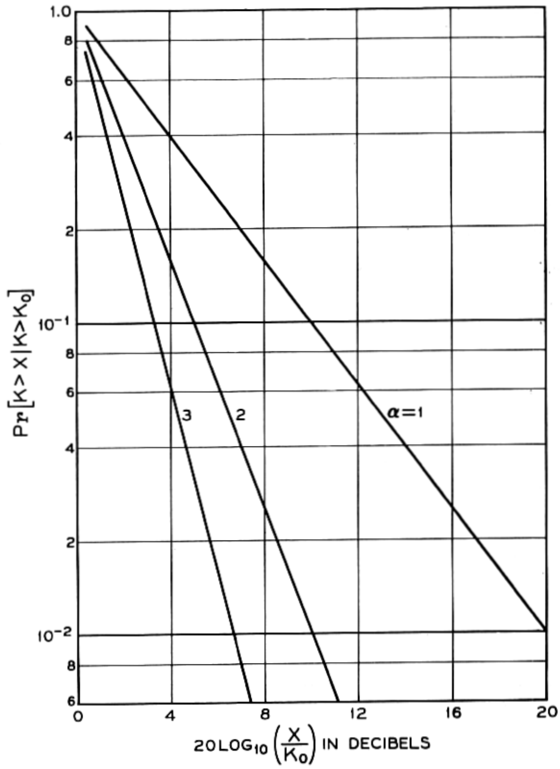

Fig. 2 — Distribution of noise burst amplitudes.

and 2.5, with occasional higher values. High values of α correspond to channels with a small percentage of high amplitude bursts, and thus result in low conditional error rates. Lower values of α correspond to channels with a greater percentage of high amplitude bursts, resulting in higher conditional error rates. A distribution with α equal to 1 would have an infinite variance; the mean of K^2, which is the average energy in a noise burst, would be infinite. A value of 1 is a lower bound on α, resulting in an upper bound on the conditional error rate.

A function which is more useful in the ensuing analysis is the distribution of the energies of the noise bursts. Since the envelope function is normalized such that this energy ε is equal to K^2, letting $y = x^2$ and $\varepsilon_0 = K_0^2$ yields:

$$Q(y) = \Pr[\varepsilon > y] = (\varepsilon_0/y)^\alpha \quad \text{for} \quad y > \varepsilon_0 \tag{5}$$

where $\mathcal{E}_0$ is the energy of the lowest energy noise burst included in the distribution.

The result of the ensuing analysis is the calculation of the conditional error rate, in terms of the average number of errors per noise burst, as a function of a signal-to-noise ratio. This ratio is defined as the average signal energy per data bit divided by the minimum burst energy $\mathcal{E}_0$. For a given modulation system and signal power, a value of $\mathcal{E}_0$ may be chosen that is sufficiently low to insure that all noise bursts which cause errors must have greater energy. Then for any given channel, an impulse counter with its threshold set to count impulses with energy greater than $\mathcal{E}_0$ can find the number of such noise bursts per data bit transmitted. The product of this number and the conditional error rate is then the over-all error rate, in bits in error per bit transmitted.

The second random variable associated with each noise burst is the phase ψ of the carrier, which is assumed to be uniformly distributed in the interval between 0 and 2π.

The third random variable associated with each noise burst is the time of occurrence. Let the sampling instant for an arbitrarily chosen data pulse be designated as the time origin $t = 0$, and let the time of occurrence of the closest noise burst, past or future, be designated as $t = \tau$. It is assumed that the average interval between noise bursts is so much greater than the duration of the bursts, that the probability of two of them overlapping is negligibly small. Then, if an error does occur due to noise at the sampling instant $t = 0$, only the nearest burst, occurring at $t = \tau$, has contributed toward it. For the average rates at which the noise bursts have been observed to occur, this assumption is valid.

For the purposes of the subsequent analyses, the density function $p(\tau)$ is only of interest for absolute values of τ less than the duration of the noise burst. If the closest noise burst occurs at a time τ which is more than a noise burst duration removed from the sampling instant, then no remnant of the noise is present at the sampling instant, and hence no error can occur. This duration is so short compared to the average interval between bursts that $p(\tau)$ is essentially constant, equal to $p(0)$, over that range of values. Further, for the distributions which have been measured, $p(0)$ is approximately equal to the average number of bursts, per unit time, β, of greater energy than $\mathcal{E}_0$. (This can be shown to be exactly true for the case when the intervals are exponentially distributed, with a Poisson distribution for the number of noise bursts occurring in a given period. It is very nearly true for the other distributions proposed.) For absolute values of τ greater than the duration of the noise burst, the density function $p(\tau)$ does not enter the analysis, and no further assumptions are required.

In the following sections, the various modulation systems are analyzed, and their performance in the presence of the noise described above is determined.

III. AMPLITUDE MODULATION SYSTEMS

3.1 *Double-Sideband AM with Coherent Detection*

The ideal data receiver using coherent detection consists of a band-pass filter $H_c(\omega)$, followed by a coherent detector and a post-detection low pass filter $H_L(\omega)$. When double sideband transmission is utilized, the band-pass filter is symmetrical about the carrier frequency ω_c. The detector multiplies the received signal by a carrier signal with the same frequency and phase as that of the modulated carrier at the transmitter. The post-detection filter removes those components of the resulting signal centered about $|\omega| = 2\omega_c$, in addition to shaping the resulting baseband signal. The post-detection filter is followed by a synchronous decision device which samples its input at discrete sampling instants T seconds apart. A block diagram of the receiver is shown in Fig. 3.

At the input to the decision device, the data signal $y(t)$ consists of a sequence of identical, except for polarity, pulses $y_0(t)$ spaced T seconds apart

$$y(t) = \sum_i a_i E y_0(t - iT) \tag{6}$$

where a_i equals $+1$ if the ith bit is a mark, and -1 if it is a space. At the jth sampling instant $t = jT$, the data signal $y(jT)$ should equal $a_j E$ with no intersymbol interference present from any other pulse. The signal $y_0(t)$ is band limited and cannot be restricted to a time slot T seconds in width. Each pulse extends over several sampling instants. In order to avoid intersymbol interference, $y_0(t)$ is constrained to be a

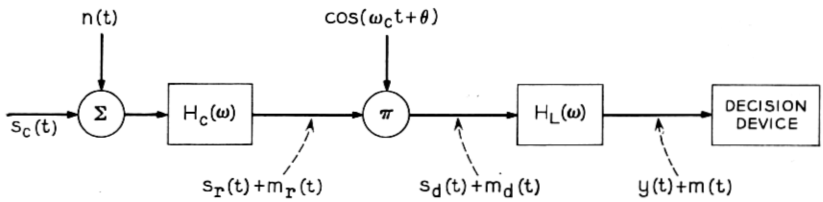

Fig. 3 — AM receiver with coherent detection.

member of a class of functions equal to 1 at $t = 0$ and equal to zero at all other integral multiples of T, satisfying Nyquist's First Criterion.[8]

In the absence of noise, each sample may have one of only two possible values. The ith sample may be $\pm E$, depending on whether the ith bit is a mark or a space. When noise is present, the sample may have one of a range of values. The decision device is a maximum likelihood estimator, producing a mark symbol if the sample value is positive, and a space symbol if it is negative. At any sampling instant, the noise will cause an error if it has an absolute value greater than E and polarity opposite to that of the data signal. The probability of this event occurring, as a function of the signal-to-noise ratio, will now be found.

Let $t = 0$ denote the sampling instant for an arbitrarily chosen data pulse, and let $t = \tau$ denote the time of occurrence of the closest noise burst. As discussed, the probability of two bursts overlapping is negligibly small. If an error does occur at the sampling instant, it is the result only of the closest noise burst. As described in Section II, the noise burst $n(t)$ is given by (1), and has a spectrum given by

$$N(\omega) = (K/2)\{e^{j\psi}N_0(\omega - \omega_c) \exp[-j(\omega - \omega_c)\tau] + e^{-j\psi}N_0(\omega + \omega_c) \exp[-j(\omega + \omega_c)\tau]\}. \tag{7}$$

The spectrum of the noise at the output of the post-detection filter $H_L(\omega)$ is

$$M(\omega) = (K/4)N_0(\omega)[e^{j(\psi-\theta)}H_c(\omega + \omega_c) + e^{-j(\psi-\theta)}H_c(\omega - \omega_c)]e^{-j\omega\tau}H_L(\omega). \tag{8}$$

As described, the band-pass filter $H_c(\omega)$ is symmetrical about the carrier frequency $|\omega| = \omega_c$, therefore,

$$H_c(\omega + \omega_c)H_L(\omega) = H_c(\omega - \omega_c)H_L(\omega).$$

An "equivalent receiving filter" $H(\omega)$ is now defined as

$$H(\omega) \triangleq H_c(\omega + \omega_c)H_L(\omega) = H_c(\omega - \omega_c)H_L(\omega), \tag{9}$$

so that

$$M(\omega) = (K/2) \cos \phi N_0(\omega)H(\omega) \exp(-j\omega\tau) \tag{10}$$

where $\phi = \psi - \theta$ is uniformly distributed in the interval between 0 and 2π. Let $m_0(t)$ be defined as the response of the equivalent receiving filter $H(\omega)$ to the normalized envelope $n_0(t)$, given by

$$m_0(t) = \frac{1}{2\pi}\int_{-\infty}^{\infty} N_0(\omega)H(\omega) \exp(j\omega t)\, d\omega. \tag{11}$$

Then, at the output of the post-detection filter, the noise has the spectrum

$$M(\omega) = (K/2) \cos \phi \, M_0(\omega) \exp(-j\omega\tau). \tag{12}$$

At the sampling instant $t = 0$, the noise at the input to the decision device is equal to

$$m(0) = (K/2) \cos \phi m_0(-\tau). \tag{13}$$

An error will occur if the absolute value of $m(0)$ is greater than E and if the polarity of the noise is opposite to that of the signal. The probability of error at the sampling instant $t = 0$, given that the closest noise burst has occurred at $t = \tau$ with relative phase ϕ, is thus equal to

$$\Pr[\text{error} \mid \tau,\phi] = \tfrac{1}{2} \Pr[m^2(0) > E^2 \mid \tau,\phi]. \tag{14}$$

Substituting the right-hand side of (13) for $m(0)$, a rearrangement of terms yields

$$\Pr[\text{error} \mid \tau,\phi] = \tfrac{1}{2} \Pr\left[\varepsilon > \frac{4E^2}{\cos^2 \phi m_0^2(-\tau)} \mid \tau,\phi\right]. \tag{15}$$

By (5), this is

$$\Pr[\text{error} \mid \tau,\phi] = \frac{1}{2}\left[\frac{\varepsilon_0 \cos^2 \phi m_0^2(-\tau)}{4E^2}\right]^\alpha. \tag{16}$$

The relative phase ϕ is uniformly distributed in the interval between 0 and 2π. Therefore, the probability of error at the sampling instant $t = 0$, given that the closest noise burst has occurred at $t = \tau$, is given by

$$\Pr[\text{error} \mid \tau] = \frac{C_\alpha}{2}\left[\frac{\varepsilon_0 m_0^2(-\tau)}{4E^2}\right]^\alpha, \tag{17}$$

where

$$C_\alpha = \frac{1}{2\pi}\int_0^{2\pi} (\cos^2 \phi)^\alpha \, d\phi. \tag{18}$$

The probability of error, at any arbitrary sampling instant, is

$$\Pr[\text{error}] = \frac{C_\alpha}{2}\left[\frac{\varepsilon_0}{4E^2}\right]^\alpha \int_{-\infty}^{\infty} m_0^{2\alpha}(-\tau) p(\tau) \, d\tau. \tag{19}$$

The density function $p(\tau)$ is only of interest for the range of τ less than the duration of the noise burst $m_0(t)$. For larger values of τ, $m_0^{2\alpha}(-\tau)$ is essentially equal to zero, and the integrand in (19) is zero. As described in the discussion of the noise model, the density function is essentially constant and equal to the average number of bursts per unit time β, for the range of τ of interest. The probability of error is therefore essentially equal to

$$\Pr[\text{error}] = \frac{\beta C_\alpha}{2}\left[\frac{\varepsilon_0}{4E^2}\right]^\alpha \int_{-\infty}^{\infty} m_0^{2\alpha}(-\tau)\, d\tau. \tag{20}$$

The system is constrained to operate with a limitation on the average power of the signal on the channel. Under such a limitation, the error rate should be given as a function of the average power of the transmitted signal, rather than of the peak value E. It may be shown that for the double-sideband amplitude modulated signal $s_c(t)$, which yields the signal $y(t)$ given by (6), the average power on the channel is

$$\bar{W} = \frac{E^2}{\pi T}\int_{-\infty}^{\infty}\left|\frac{Y_0(\omega)}{H(\omega)}\right|^2 d\omega \tag{21}$$

where $Y_0(\omega)$ is the spectrum of the individual data pulse $y_0(t)$. Let I_1 be defined as the integral

$$I_1 \triangleq \frac{1}{2\pi T}\int_{-\infty}^{\infty}\left|\frac{Y_0(\omega)}{H(\omega)}\right|^2 d\omega. \tag{22}$$

Then substituting in (21) and (22) into (20),

$$\Pr[\text{error}] = \frac{\beta C_\alpha}{2}\left[\frac{\varepsilon_0 I_1}{2\bar{W}}\right]^\alpha \int_{-\infty}^{\infty} m_0^{2\alpha}(-\tau)\, d\tau. \tag{23}$$

Substituting $t = -\tau$ in the definite integral and rearranging some of the terms, (23) yields

$$\Pr[\text{error}] = \frac{\beta C_\alpha T}{2}\left[\frac{1}{2}I_1\frac{\varepsilon_0}{\bar{W}T}\right]^\alpha \int_{-\infty}^{\infty} [T m_0^2(t)]^\alpha \frac{dt}{T}, \tag{24}$$

where $\bar{W}T/\varepsilon_0$ is the signal-to-noise ratio defined previously as the signal energy per bit divided by the energy in the minimum noise burst. The rearrangement of terms in the above expression normalizes the integral to a dimensionless constant.

Since $Y_0(\omega)$ is specified by the system designer, and $N_0(\omega)$ is known, the equivalent receiving filter characteristic $H(\omega)$ may be optimized in the sense that the probability of error is minimized. For each value of α, however, a different characteristic is optimum. Since the data system is to be used over randomly selected channels, with all possible values of α, it appears reasonable that it should be optimized in a minimax sense.

The system design should therefore be optimized for the worst case, which corresponds to a value of α equal to 1. If the system then operates with an acceptably low error rate over a channel with a value of α equal to 1, it will operate with an even lower error rate over another channel with a higher value of α. The optimization procedure therefore consists of finding the filter characteristic which minimizes the probability of error for a value of α equal to one. For that case, the probability of error is equal to

$$\Pr[\text{error}] = \frac{\beta}{16\pi} \frac{\varepsilon_0}{\bar{W}T} \int_{-\infty}^{\infty} \left| \frac{Y_0(\omega)}{H(\omega)} \right|^2 d\omega \int_{-\infty}^{\infty} m_0^2(t)\, dt \tag{25}$$

where, by Parseval's theorem

$$\begin{aligned} \int_{-\infty}^{\infty} m_0^2(t)\, dt &= \frac{1}{2\pi} \int_{-\infty}^{\infty} |\, M_0(\omega)\,|^2\, d\omega \\ \int_{-\infty}^{\infty} m_0^2(t)\, dt &= \frac{1}{2\pi} \int_{-\infty}^{\infty} |\, N_0(\omega) H(\omega)\,|^2\, d\omega. \end{aligned} \tag{26}$$

Then

$$\Pr[\text{error}] = \frac{1}{32\pi^2} \left[\frac{\varepsilon_0}{\bar{W}T} \right] \int_{-\infty}^{\infty} \left| \frac{Y_0(\omega)}{H(\omega)} \right|^2 d\omega \int_{-\infty}^{\infty} |\, N_0(\omega) H(\omega)\,|^2\, d\omega. \tag{27}$$

By Schwarz's inequality

$$\left| \int_{-\infty}^{\infty} Y_0(\omega) N_0(\omega)\, d\omega \right|^2 \leqq \int_{-\infty}^{\infty} \left| \frac{Y_0(\omega)}{H(\omega)} \right|^2 d\omega \int_{-\infty}^{\infty} |\, N_0(\omega) H(\omega)\,|^2\, d\omega. \tag{28}$$

The equality is satisfied when

$$\frac{Y_0(\omega)}{H(\omega)} = C N_0^*(\omega) H^*(\omega) \tag{29}$$

where C is any real constant and the asterisk denotes the complex conjugate. Since the left hand side of the inequality is independent of $H(\omega)$, it represents the minimum value the right hand side may take. The probability of error is therefore minimized when the equality is satisfied, and this occurs when the filter characteristic satisfies the relation

$$|\, H(\omega)\,|^2 = \frac{1}{C} \frac{Y_0(\omega)}{N_0^*(\omega)} \,. \tag{30}$$

The phase characteristic of $H(\omega)$ has no effect on the probability of error for the limiting case when α is equal to 1. The system performance is therefore evaluated for zero (or linear) phase shift. The phase characteristic does affect the error probability when α is greater than 1; this effect is considered in detail in a subsequent section on complementary delay filters.

The probability of error is dependent on two parameters of the noise bursts, the distribution of their amplitudes-defined by α, and their relative frequency — defined by β. This second dependence consists merely of a direct proportionality, and need not be carried along in the computation. The performance measure may be normalized by considering the conditional error rate, defined as the average number of bit errors per noise burst. The probability of error is equal to the average number of bit errors per bit transmitted. If this number is divided by the average number of noise bursts per bit transmitted, βT, the result is the average number of bit errors per noise burst,

$$\bar{N} = \frac{\Pr[\text{error}]}{\beta T}.$$

given by:

$$\bar{N} = \frac{C_\alpha}{2}\left[\frac{1}{2} I_1 \frac{\varepsilon_0}{\bar{W}T}\right]^\alpha \int_{-\infty}^{\infty} [Tm_0^2(t)]^\alpha \frac{dt}{T}. \tag{31}$$

In order to obtain some numerical results, the general expression for $\bar{N}$ given above is to be evaluated for a special case which is of interest. In the transmission of data over narrow-band telephone channels, the spectrum of the individual data pulses $y_0(t)$ is often the "raised cosine" spectrum given by

$$Y_0(\omega) = (T/2)[1 + \cos(\omega T/2)] \quad \text{for} \quad |\omega| < 2\pi/T. \tag{32}$$

This signal satisfies all three of Nyquist's criteria:

(1.) $y_0(iT) = \begin{matrix} 1 \text{ for } i = 0 \\ 0 \text{ for } i = 1, 2, 3, \cdots . \end{matrix}$

(2.) $y_0[i(T/2)] = \begin{matrix} \frac{1}{2} \text{ for } i = 1 \\ 0 \text{ for } i = 2, 3, 4, \cdots . \end{matrix}$

(3.) The envelope of $y_0(t)$ approaches zero very rapidly as $|t|$ increases.

For the sake of simplicity it will be assumed that in the narrow band of interest $|\omega| < 2\pi/T$, the spectrum of the noise $N_0(\omega)$ is constant. Since the energy of the noise burst $n_0(t)$ in the band of interest is equal to 2 watt-seconds, the noise spectrum is given by

$$N_0(\omega) = \sqrt{T} \quad \text{for} \quad |\omega| < 2\pi/T. \tag{33}$$

The optimum filter characteristic is given by

$$H(\omega) = \{\tfrac{1}{2}[1 + \cos(\omega T/2)]\}^{\frac{1}{2}} \quad \text{for} \quad |\omega| < 2\pi/T$$
$$H(\omega) = \cos(\omega T/4) \quad \text{for} \quad |\omega| < 2\pi/T. \tag{34}$$

Note that the optimization permitted an arbitrary scale factor for $H(\omega)$, since signal and noise would be identically affected. This scale factor has been chosen such that the maximum value of $H(\omega)$ is unity.

The expression for $\bar{N}$ has been numerically evaluated on a digital computer, for values of α equal to 1, 2, and 3, chosen to be representative. The results are tabulated here, and are plotted in Fig. 4.

α	$\bar{N}$
1	$0.124\ \mathcal{E}_0/\bar{W}T$
2	$0.0545\ (\mathcal{E}_0/\bar{W}T)^2$
3	$0.0302\ (\mathcal{E}_0/\bar{W}T)^3$

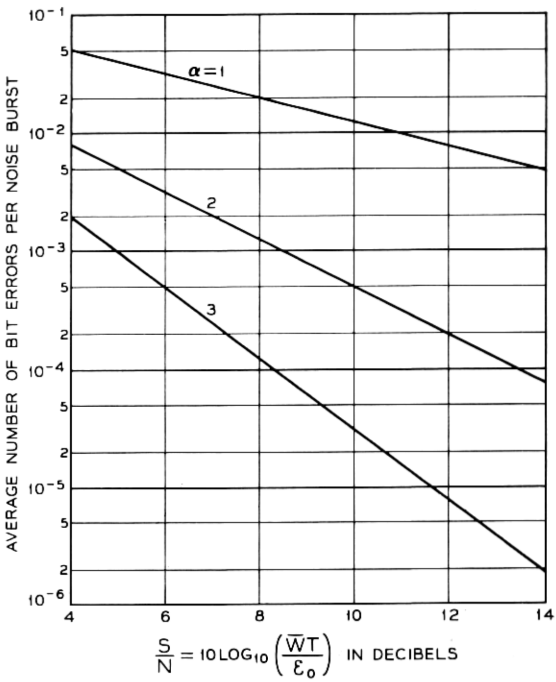

Fig. 4 — Performance of double-sideband AM system with coherent detection.

3.2 *Single-Sideband AM with Coherent Detection*

The ideal data receiver has the same form as the one described in the previous section. The only difference is that when single-sideband transmission is utilized, the band-pass filter $H_c(\omega)$ does not pass frequencies below ω_c

$$H_c(\omega) = 0 \quad \text{for} \quad |\omega| < \omega_c . \tag{35}$$

At frequencies above ω_c, the band-pass filter is identical to that for the double-sideband case.

As in the previous analysis, let $t = 0$ denote the sampling instant for an arbitrarily chosen data pulse, and let $t = \tau$ denote the time of occurrence of the closest noise burst. As in the double-sideband case, the spectrum of the noise burst at the output of the post-detection filter is given by (8). However, since $H_c(\omega)$ is equal to zero for all $|\omega|$ less than ω_c, this spectrum is equal to

$$M(\omega) = (K/4)M_0(\omega)\,[\cos\phi + j\,sgn(\omega)\sin\phi]\exp(-j\omega\tau), \tag{36}$$

and the noise burst is

$$m(t) = (K/4)[m_0(t-\tau)\cos\phi - \hat{m}_0(t-\tau)\sin\phi]$$

where $\hat{m}_0(t)$ is the Hilbert transform of $m_0(t)$, given by:

$$\hat{m}_0(t) = \frac{1}{2\pi}\int_{-\infty}^{\infty}\frac{1}{j}\,sgn(\omega)N_0(\omega)H(\omega)\exp(j\omega t)\,d\omega. \tag{37}$$

At the sampling instant $t = 0$, the noise at the input to the decision device is equal to

$$m(0) = (K/4)[m_0(-\tau)\cos\phi - \hat{m}_0(-\tau)\sin\phi]. \tag{38}$$

Substituting the right-hand side of (38) for $m(0)$ in the expression for the probability of error, (14), and rearranging terms,

$$\Pr[\text{error} \mid \tau,\phi] = \tfrac{1}{2}\Pr\left\{\varepsilon > \frac{16E^2}{[m_0(-\tau)\cos\phi - \hat{m}_0(-\tau)\sin\phi]^2}\,\middle|\,\tau,\phi\right\}. \tag{39}$$

By (5), this is equal to

$$\Pr[\text{error} \mid \tau,\phi] = \frac{1}{2}\left\{\frac{\varepsilon_0[m_0(-\tau)\cos\phi - \hat{m}_0(-\tau)\sin\phi]^2}{16E^2}\right\}^{\alpha}, \tag{40}$$

and may be rewritten in the form

$$\Pr[\text{error} \mid \tau,\phi] = \frac{1}{2}\left[\frac{\varepsilon_0}{16E^2}\right]^\alpha [m_0^2(-\tau) + \hat{m}_0^2(-\tau)]^\alpha (\cos^2 \chi)^\alpha \quad (41)$$

where, for any given value of τ, the angle

$$\chi = \phi + \tan^{-1} \frac{\hat{m}_0(-\tau)}{m_0(-\tau)} \quad (42)$$

is uniformly distributed in the interval between 0 and 2π. Averaging (41) with respect to χ and τ yields

$$\Pr[\text{error}] = \frac{\beta C_\alpha}{2}\left[\frac{\varepsilon_0}{16E^2}\right]^\alpha \int_{-\infty}^{\infty} [m_0^2(-\tau) + \hat{m}_0^2(-\tau)]^\alpha \, d\tau. \quad (43)$$

It may be shown that, for the single-sideband amplitude-modulated signal $s_c(t)$ which yields the signal $y(t)$ given by (6), the average power on the channel is equal to

$$\bar{W} = 4E^2 I_1 \quad (44)$$

where I_1 is the integral defined by (22). Substituting (44) in (43) and rearranging some of the terms yields:

$$\Pr[\text{error}] = \frac{\beta C_\alpha T}{2}\left[\frac{1}{4} I_1 \frac{\varepsilon_0}{\bar{W}T}\right]^\alpha \int_{-\infty}^{\infty} [Tm_0^2(t) + T\hat{m}_0^2(t)]^\alpha \frac{dt}{T} \quad (45)$$

where $\bar{W}T/\varepsilon_0$ is the signal-to-noise ratio defined previously.

In the same manner as for the double-sideband system, the equivalent receiving filter characteristic $H(\omega)$ is designed to minimize the probability of error for the case when α is equal to 1. For that value of α, the error probability is given by

$$\Pr[\text{error}] = \frac{\beta}{32\pi}\left[\frac{\varepsilon_0}{\bar{W}T}\right] \int_{-\infty}^{\infty} \left|\frac{Y_0(\omega)}{H(\omega)}\right|^2 d\omega \left[\int_{-\infty}^{\infty} m_0^2(t)\, dt + \int_{-\infty}^{\infty} \hat{m}_0^2(t)\, dt\right]. \quad (46)$$

By Parseval's theorem

$$\int_{-\infty}^{\infty} m_0^2(t)dt = \int_{-\infty}^{\infty} \hat{m}_0^2(t)\,dt = \frac{1}{2\pi}\int_{-\infty}^{\infty} | N_0(\omega)H(\omega) |^2 \, d\omega. \quad (47)$$

Substituting (47) into (46) yields the same expression as for the double-sideband case, given by (27). The optimum filter characteristic is therefore the same, satisfying (30).

The conditional error rate, defined as the average number of bit errors per noise burst, is given by

$$\bar{N} = \frac{C_\alpha}{2}\left[\frac{1}{4} I_1 \frac{\varepsilon_0}{\bar{W}T}\right]^\alpha \int_{-\infty}^{\infty} [Tm_0^2(t) + T\hat{m}_0^2(t)]^\alpha \frac{dt}{T}. \qquad (48)$$

In order to obtain numerical results, the general expression for $\bar{N}$ is evaluated for the special case described previously. The spectrum of an individual data pulse is the raised cosine spectrum, and the noise spectrum is assumed to be constant in the band of interest. The expression for $\bar{N}$ has been numerically evaluated for values of α equal to 1, 2 and 3. The results are tabulated here, and are plotted in Fig. 5.

α	$\bar{N}$
1	$0.124\ (\varepsilon_0/\bar{W}T)$
2	$0.0241\ (\varepsilon_0/\bar{W}T)^2$
3	$0.0069\ (\varepsilon_0/\bar{W}T)^3$

3.3 *AM with Envelope Detection*

The ideal data receiver using envelope detection consists of a receiving filter $H_c(\omega)$, symmetrical about the carrier frequency ω_c, followed by

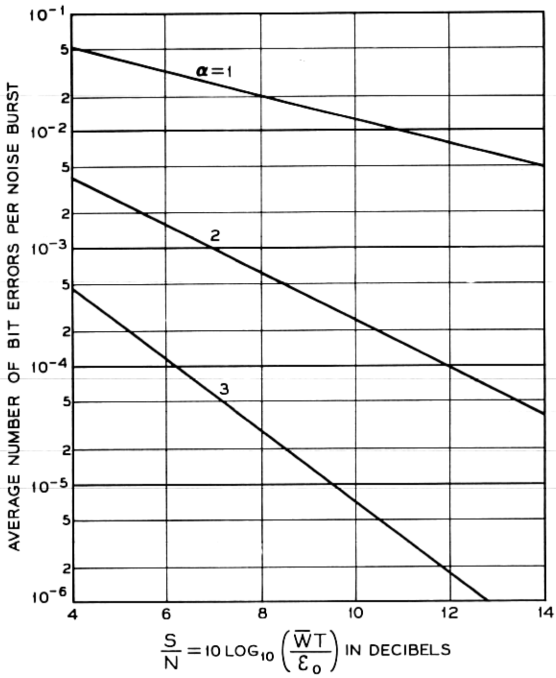

Fig. 5 — Performance of single-sideband AM system with coherent detection.

an ideal envelope detector. The output of the envelope detector is applied to a synchronous decision device. A block diagram of the receiver is shown in Fig. 6. The signal $y(t)$ at the input to the decision device has the form of (6). At the ith sampling instant, it is equal to

$$y(iT) = | a_i |.$$

Since polarity information is lost, and only magnitude information is delivered to the decision device, unipolar signaling must be used. If the ith bit is a mark, a_i is equal to $+1$; if the ith bit is a space, a_i is equal to zero. The threshold of the decision logic is set at a level λE, where λ has a value between zero and one. If the ith sample is greater than λE, a mark symbol is produced; if less than λE, a space symbol is produced. The value of λ is chosen to minimize the probability of error in the presence of noise.

Let $t = 0$ denote the sampling instant for an arbitrarily chosen data pulse, and let $t = \tau$ denote the time of occurrence of the closest noise burst. The noise burst on the channel is given by (1). At the input to the detector, the noise burst is given by

$$m_r(t) = Km_0(t - \tau)[\cos \phi \cos (\omega_c t + \theta) - \sin \phi \sin (\omega_c t + \theta)] \quad (49)$$

where the previously described phase difference

$$\phi = \psi - \theta,$$

is uniformly distributed in the interval between 0 and 2π.

At the input to the detector, the combined signal and noise voltage is equal to

$$v_i(t) = [y_r(t) + Km_0(t - \tau) \cos \phi] \cos (\omega_c t + \theta) - Km_0(t - \tau) \sin \phi \sin (\omega_c t + \theta). \quad (50)$$

The detector output is

$$v_0(t) = \sqrt{[y_r(t) + Km_0(t - \tau) \cos \phi]^2 + [Km_0(t - \tau) \sin \phi]^2}. \quad (51)$$

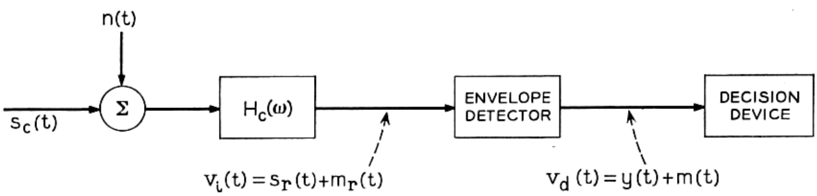

Fig. 6 — AM receiver with envelope detection.

If, at the sampling instant $t = 0$, a space has been sent, the voltage at the input to the decision device is equal to the noise alone

$$v_0(0) = |Km_0(-\tau)|. \tag{52}$$

An error will occur if this magnitude is greater than λE. The probability of error at the sampling instant $t = 0$, given that a space has been sent and that the closest noise burst has occurred at $t = \tau$, is therefore equal to

$$\Pr[\text{error} \mid \text{space}, \tau] = \Pr[\varepsilon m_0^2(-\tau) > \lambda^2 E^2 \mid \tau] \tag{53}$$

and, by (5), this is

$$\Pr[\text{error} \mid \text{space}, \tau] = \left[\frac{\varepsilon_0 m_0^2(-\tau)}{\lambda^2 E^2}\right]^\alpha \tag{54}$$

If, at the sampling instant $t = 0$, a mark has been sent, the voltage at the input to the decision device is equal to

$$v_0(0) = +\sqrt{[E + Km_0(-\tau)\cos\phi]^2 + [Km_0(-\tau)\sin\phi]^2} \tag{55}$$

and an error will occur if this is less than λE. This is shown graphically in the phasor diagrams of Fig. 7. An error will occur if the vector sum of the signal E and the noise $Km_0(-\tau)$ making an angle ϕ with E falls within the circle of radius λE.

Fig. 7(a) shows the phasor diagram when $m_0(-\tau)$ is positive. An error can occur only for values of ϕ in the interval

$$\pi + \sin^{-1}\lambda \geqq \phi \geqq \pi - \sin^{-1}\lambda.$$

For all other values of ϕ the vector sum cannot fall within the circle. When ϕ is within the above interval, an error will occur if $Km_0(-\tau)$

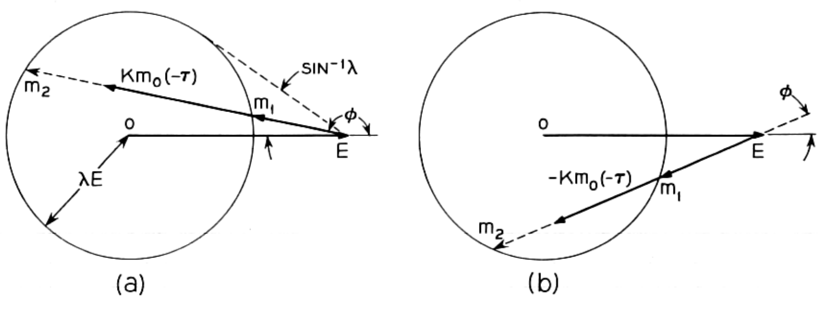

Fig. 7 — (a) Phasor diagram when $m_0(-\tau)$ is positive. (b) Phasor diagram when $m_0(-\tau)$ is negative.

lies in the interval

$$m_2 > Km_0(-\tau) > m_1 \tag{56}$$

where m_1 and m_2 are functions of ϕ. By the Law of Cosines, m_1 and m_2 must satisfy

$$\lambda^2 E^2 = E^2 + m^2 - 2mE \cos (\pi - \phi), \tag{57}$$

hence,

$$\begin{aligned} m_1 &= \frac{(1-\lambda^2)E}{\cos(\pi-\phi) + \sqrt{\lambda^2 - \sin^2(\pi-\phi)}} \\ m_2 &= \frac{(1-\lambda^2)E}{\cos(\pi-\phi) - \sqrt{\lambda^2 - \sin^2(\pi-\phi)}}. \end{aligned} \tag{58}$$

The probability of error at the sampling instant $t = 0$, given that a mark has been sent and that the closest noise burst has occurred at $t = \tau$, such that $m_0(-\tau) > 0$, with phase difference ϕ, is equal to the probability that the noise is within the range (56), and is

$$\begin{aligned} &\Pr[\text{error} \mid \text{mark}, \tau, m_0(-\tau) > 0, \phi] \\ &\quad = \Pr\left[\frac{m_2^2}{m_0^2(-\tau)} > \varepsilon > \frac{m_1^2}{m_0^2(-\tau)} \,\middle|\, \tau, \phi \right] \\ &\qquad \text{for} \quad \pi + \sin^{-1}\lambda > \phi > \pi - \sin^{-1}\lambda \end{aligned} \tag{59}$$

and is equal to zero for all other values of ϕ. By (5) this is equal to

$$\begin{aligned} &\Pr[\text{error} \mid \text{mark}, \tau, m_0(-\tau) > 0, \phi] \\ &= \left\{ \frac{\varepsilon_0 m_0^2(-\tau)[\cos(\pi-\phi) + \sqrt{\lambda^2 - \sin^2(\pi-\phi)}]^2}{(1-\lambda^2)^2 E^2} \right\}^{\alpha} \\ &\quad - \left\{ \frac{\varepsilon_0 m_0^2(-\tau)\,[\cos(\pi-\phi) - \sqrt{\lambda^2 - \sin^2(\pi-\phi)}]^2}{(1-\lambda^2)^2 E^2} \right\}^{\alpha} \\ &\quad \text{for} \quad \pi + \sin^{-1}\lambda > \phi > \pi - \sin^{-1}\lambda. \end{aligned} \tag{60}$$

The phase difference ϕ is uniformly distributed in the interval between 0 and 2π. Therefore, averaging (60) with respect to ϕ yields:

$$\begin{aligned} &\Pr[\text{error} \mid \text{mark}, \tau, m_0(-\tau) > 0] \\ &= \frac{1}{\pi}\left[\frac{\varepsilon_0 m_0^2(-\tau)}{(1-\lambda^2)^2 E^2} \right]^{\alpha} \int_0^{\sin^{-1}\lambda} \{[\cos\phi + \sqrt{\lambda^2 - \sin^2\phi}]^{2\alpha} \\ &\quad - [\cos\phi - \sqrt{\lambda^2 - \sin^2\phi}]^{2\alpha}\}\, d\phi. \end{aligned} \tag{61}$$

Fig. 7(b) shows the phasor diagram when $m_0(-\tau)$ is negative. By reasoning similar to that presented above, it can be shown that the probability of error at the sampling instant $t = 0$, given that a mark has been sent and that the closest noise burst has occurred at $t = \tau$, such that $m_0(-\tau) < 0$, is also given by (61). The probability of error given that $m_0(-\tau)$ is positive is identically equal to the probability of error given that it is negative. Since the two events are disjoint

$$\Pr[\text{error} \mid \text{mark}, \tau] = \frac{1}{\pi}\left[\frac{\varepsilon_0 m_0^2(-\tau)}{(1-\lambda^2)^2 E^2}\right]^\alpha \int_0^{\sin^{-1}\lambda} \{[\cos\phi + \sqrt{\lambda^2 - \sin^2\phi}]^{2\alpha} - [\cos\phi - \sqrt{\lambda^2 - \sin^2\phi}]^{2\alpha}\}\, d\phi. \tag{62}$$

Marks and spaces are assumed to occur with equal probability. Therefore, the probability of error at the sampling instant $t = 0$, given that the closest noise burst has occurred at $t = \tau$, is equal to one-half the sum of (54) and (62). Let a signal-to-noise ratio coefficient be defined by

$$f_\alpha(\lambda) = \left\{\frac{1}{\lambda^{2\alpha}} + \frac{1}{\pi(1-\lambda^2)^{2\alpha}} \int_0^{\sin^{-1}\lambda} \{[\cos\phi + \sqrt{\lambda^2 - \sin^2\phi}]^{2\alpha} - [\cos\phi - \sqrt{\lambda^2 - \sin^2\phi}]^{2\alpha}\}\, d\phi\right\}^{1/\alpha}. \tag{63}$$

Then, the probability of error, given τ, equals

$$\Pr[\text{error} \mid \tau] = \frac{1}{2}\left[\frac{f_\alpha(\lambda)\varepsilon_0 m_0^2(-\tau)}{E^2}\right]^\alpha. \tag{64}$$

As shown previously, averaging with respect to τ yields that the probability of error at any arbitrary sampling instant is essentially equal to:

$$\Pr[\text{error}] = \frac{\beta}{2}\left[\frac{f_\alpha(\lambda)\varepsilon_0}{E^2}\right]^\alpha \int_{-\infty}^{\infty} m_0^{2\alpha}(-\tau)\, d\tau. \tag{65}$$

The value of the threshold level λ is to be selected to minimize the coefficient $f_\alpha(\lambda)$. The functions $f_\alpha(\lambda)$ and $df_\alpha(\lambda)/d\lambda$ have been evaluated for values of α equal to 1, 2, and 3. These are plotted in Figs. 8 and 9, respectively. Since a value of α equal to 1 yields the highest error rate, the threshold level λ should be selected to minimize $f_1(\lambda)$. The error rates for other values of α will always be lower than that for a value of α equal to 1. However, $f_1(\lambda)$ exhibits the broadest minimum and is most amenable to compromise. As may be seen in Fig. 8, a threshold level λ

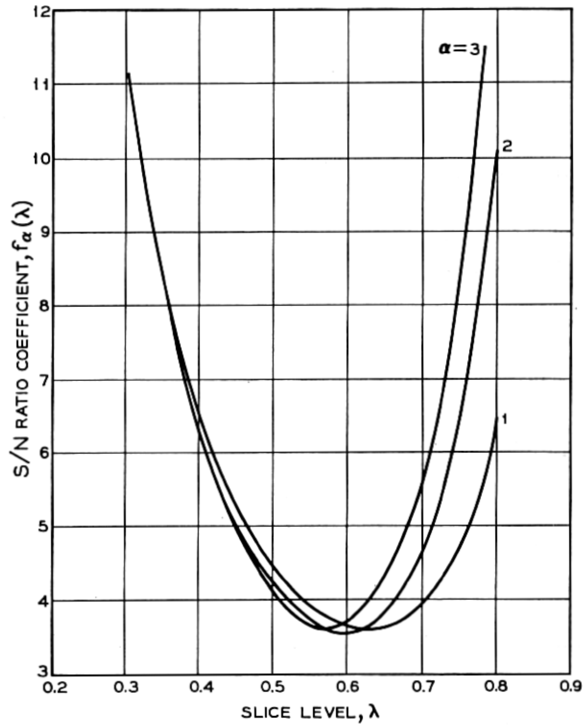

Fig. 8 — Signal-to-noise ratio coefficient.

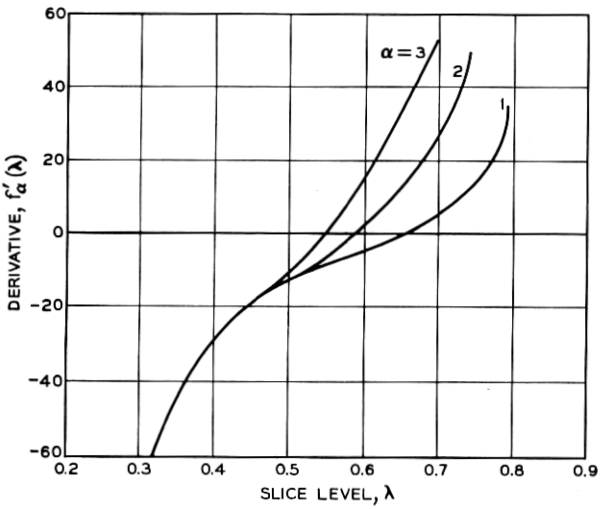

Fig. 9 — Rate of change of signal-to-noise ratio coefficient.

equal to 0.6 is a satisfactory compromise. At that value of λ, f_1 equals 3.65, f_2 equals 3.55, and f_3 equals 3.65.

It may be shown that for the unipolarly keyed modulated signal $s_c(t)$, the average power on the channel is equal to

$$\bar{W} = E^2 \left[\frac{1}{8} I_1 + \frac{1}{8T^2} \left| \frac{Y_0(0)}{H(0)} \right|^2 \right]. \tag{66}$$

The second term is recognized as the result of a carrier frequency component which is present because the average value of the baseband data signal is not equal to zero. Substituting (66) into (65) and rearranging some of the terms,

$$\Pr[\text{error}] = \frac{\beta T}{2} \left\{ \frac{f_\alpha \mathcal{E}_0 \left[I_1 + \frac{1}{T^2} \left| \frac{Y_0(0)}{H(0)} \right|^2 \right]}{8\bar{W}T} \right\}^\alpha \int_{-\infty}^{\infty} [Tm_0^2(t)]^\alpha \frac{dt}{T} \tag{67}$$

where $\bar{W}T/\mathcal{E}_0$ is the signal-to-noise ratio defined previously.

In the same manner as for the previously considered systems, the filter characteristic $H(\omega)$ is selected to minimize the error probability when α is equal to one. For that value of α, the probability of error is given by

$$\Pr[\text{error}] = \frac{\beta f_1}{(8\pi)^2} \left[\frac{\mathcal{E}_0}{\bar{W}T} \right] \int_{-\infty}^{\infty} \left| \frac{Y_0(\omega)}{H(\omega)} \right|^2 \left[1 + \frac{2\pi}{T} \delta(\omega) \right] d\omega \cdot \int_{-\infty}^{\infty} | N_0(\omega) H(\omega) |^2 \, d\omega. \tag{68}$$

By Schwarz's inequality, the above expression is minimized when the amplitude characteristic of $H(\omega)$ satisfies the relation

$$| H(\omega) |^2 \sim \frac{Y_0(\omega)}{N_0^*(\omega)} \left[1 + \frac{2\pi}{T} \delta(\omega) \right]^{\frac{1}{2}}. \tag{69}$$

The requirement of an impulse at zero frequency is equivalent to carrier suppression at the transmitter. The infinite gain at the receiver then restores the dc component of the base-band data signal. Since the construction of such a filter is not feasible, it is assumed that the filter $H(\omega)$ has the suboptimum "smooth" characteristic given by (30).

The conditional error rate, defined as the average number of bit errors per noise burst, is

$$\bar{N} = \frac{1}{2} \left\{ \frac{1}{8} f_\alpha \left[I_1 + \frac{1}{T^2} \left| \frac{Y_0(0)}{H(0)} \right|^2 \right] \frac{\mathcal{E}_0}{\bar{W}T} \right\}^\alpha \int_{-\infty}^{\infty} [Tm_0^2(t)]^\alpha \frac{dt}{T}. \tag{70}$$

In order to obtain numerical results, the general expression for $\bar{N}$ is evaluated for the special case described previously. The spectrum of an individual data pulse is the raised cosine spectrum, and the spectrum of the noise is assumed to be constant in the band of interest. The expression for $\bar{N}$ has been numerically evaluated on a digital computer, for values of α equal to 1, 2 and 3. The results are tabulated below, and are plotted in Fig. 10.

α	$\bar{N}$
1	$0.455\ (\varepsilon_0/\bar{W}T)$
2	$0.456\ (\varepsilon_0/\bar{W}T)^2$
3	$0.586\ (\varepsilon_0/\bar{W}T)^3$

IV. FREQUENCY SHIFT KEYING SYSTEM

The ideal data receiver for a frequency shift keying system consists of a receiving filter $H_c(\omega)$ which is symmetrical about the carrier frequency ω_c, followed by an ideal frequency discriminator. The output of

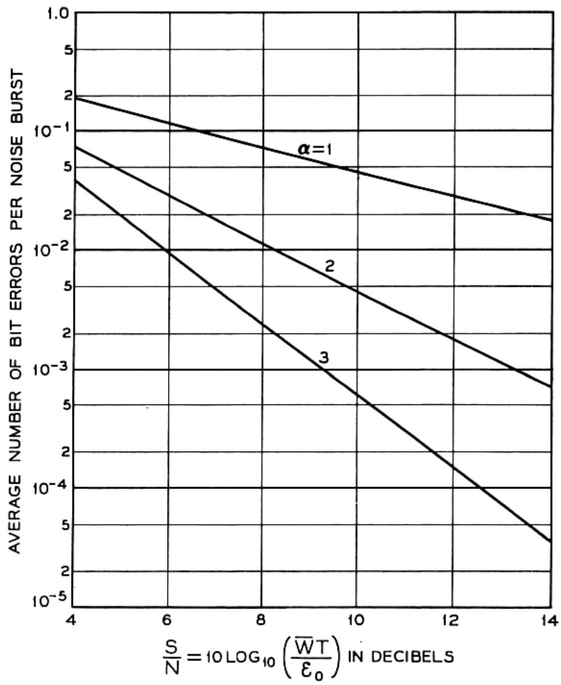

Fig. 10 — Performance of AM system with envelope detection.

the discriminator is the instantaneous frequency ω_i of the signal (plus noise) at its input. The discriminator is followed by a synchronous decision device identical to the one in the coherent AM systems. A block diagram of the receiver is shown in Fig. 11.

Sunde[9] has shown that in the absence of noise, intersymbol interference can be eliminated even though the signal at the input to the detector must be bandlimited. The frequency shift signal is generated by mixing the outputs of two synchronized oscillators; one oscillating at a mark frequency ω_m, the other at a space frequency ω_s. For this discussion, let the mark frequency be higher than the space frequency; the choice is arbitrary. The carrier frequency is defined as the mid-frequency

$$\omega_c = (\omega_m + \omega_s)/2$$

and the shift frequency is defined by:

$$2\omega_d = \omega_m - \omega_s .$$

The modulated signal is

$$s(t) = \tfrac{1}{2}\{[1 + g(t)] \cos [(\omega_c + \omega_d)t + \theta] - [1 - g(t)][\cos (\omega_c - \omega_d)t + \theta]. \quad (71)$$

At the sampling instants, the mixing function is equal to

$$g(iT) = \pm 1$$

so that the instantaneous frequency at the sampling instants is

$$\omega_i(iT) = \omega_c \pm \omega_d$$

depending on whether the ith bit is a mark or a space.

The modulated signal may be rewritten as

$$s(t) = \sin \omega_d t \sin (\omega_c t + \theta) - g(t) \cos \omega_d t \cos (\omega_c t + \theta). \quad (72)$$

After successive filtering, amplification, and transmission, the signal at the input to the discriminator, in the absence of noise, is equal to

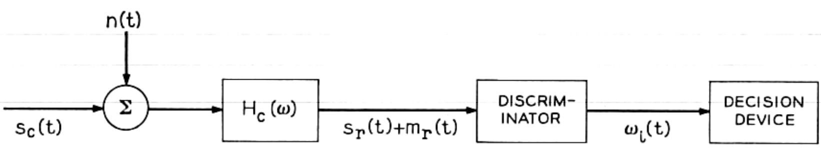

Fig. 11 — Receiver for frequency shift keyed system.

$$s_r(t) = P(t) \cos(\omega_c t + \theta) - Q(t) \sin(\omega_c t + \theta), \tag{73}$$

where

$$\begin{aligned} P(t) &= -y(t) \\ Q(t) &= -E \sin \omega_d t. \end{aligned} \tag{74}$$

As a further restriction, the shift frequency is made equal to the bit rate, so that

$$\omega_d = \pi/T$$

and

$$y(t) = \sum_i (-1)^i a_i E y_0(t - iT), \tag{75}$$

where, as before, a_i is $+1$ if the ith bit is a mark and -1 if it is a space, and $y_0(t)$ satisfies Nyquist's First Criterion. Sunde has shown that these conditions yield a signal which in the absence of noise presents no intersymbol interference.

As in the analysis of the AM systems, let $t = 0$ denote an arbitrarily selected data sampling instant, and let $t = \tau$ denote the time of occurrence of the closest noise burst. The noise at the output of the receiving filter is given by (49). With both signal and noise present at the discriminator input, the output is

$$\omega_i(t) = \frac{d}{dt}\left[\tan^{-1} \frac{Q(t) + y(t)}{P(t) + x(t)}\right] \tag{76}$$

where

$$\begin{aligned} x(t) &= K m_0(t - \tau) \cos \phi \\ y(t) &= K m_0(t - \tau) \sin \phi \end{aligned} \tag{77}$$

and is equal to

$$\omega_i(t) = \frac{[P(t) + x(t)][\dot{Q}(t) + \dot{y}(t)] - [Q(t) + y(t)][\dot{P}(t) + \dot{x}(t)]}{[P(t) + x(t)]^2 + [Q(t) + y(t)]^2}. \tag{78}$$

Since the denominator of $\omega_i(t)$ is always positive, the decision device will produce a mark if

$$\begin{aligned} V = {} & [-Ea_0 + K m_0(-\tau) \cos \phi][-(E\pi/T) + K \dot{m}_0(-\tau) \sin \phi] \\ & - [K m_0(-\tau) \sin \phi][\dot{P}(0) + K \dot{m}_0(-\tau) \cos \phi] \end{aligned} \tag{79}$$

is positive, and a space if it is negative.

For the cases of interest, it can be shown that $\dot{P}(0)$ is considerably less than $\dot{x}(0)$ for those noise bursts which cause errors. In addition, $\dot{P}(0)$ is equal to zero. For these reasons, the $\dot{P}(0)$ term is dropped in the subsequent steps, since to retain it would unnecessarily complicate the analysis.

When a mark has been sent, and a_0 is equal to $+1$, V is negative and an error occurs when

$$K[(T/\pi)\dot{m}_0(-\tau)\sin\phi + m_0(-\tau)\cos\phi] > E. \tag{80}$$

The probability of error at the sampling instant $t = 0$, given that a mark has been sent and that the closest noise burst has occurred at $t = \tau$ with phase difference ϕ, is equal to:

$$\Pr[\text{error} \mid \text{mark},\tau,\phi] = \frac{1}{2}\Pr\left\{\varepsilon^2 > \frac{E^2}{\left[\frac{T}{\pi}\dot{m}_0(-\tau)\sin\phi + m_0(-\tau)\cos\phi\right]^2}\,\middle|\,\tau,\phi\right\} \tag{81}$$

and by (5), this is equal to

$$\Pr[\text{error} \mid \text{mark},\tau,\phi] = \frac{1}{2}\left\{\frac{\varepsilon_0\left[\frac{T}{\pi}\dot{m}_0(-\tau)\sin\phi + m_0(-\tau)\cos\phi\right]^2}{E^2}\right\}^{\alpha}. \tag{82}$$

When a space has been sent, and a_0 is equal to -1, V is positive and an error occurs when:

$$K[(T/\pi)\dot{m}_0(-\tau)\sin\phi - m_0(-\tau)\cos\phi] > E. \tag{83}$$

Following the reasoning presented above, the probability of error at the sampling instant $t = 0$, given that a space has been sent and that the closest noise burst has occurred at $t = \tau$ with phase difference ϕ, is equal to

$$\Pr[\text{error} \mid \text{space},\tau,\phi] = \frac{1}{2}\left\{\frac{\varepsilon_0\left[\frac{T}{\pi}\dot{m}_0(-\tau)\sin\phi - m_0(-\tau)\cos\phi\right]^2}{E^2}\right\}^{\alpha}. \tag{84}$$

Marks and spaces occur with equal probability. Therefore, the probability of error, given τ and ϕ, is

$$\begin{aligned}\Pr[\text{error} \mid \tau,\phi] = \frac{1}{4}\left[\frac{\mathcal{E}_0}{E^2}\right]^\alpha \left\{\left[\frac{T}{\pi}\,\dot{m}_0(-\tau)\right]^2 + [m_0(-\tau)]^2\right\}^\alpha \\ \cdot\left\{\left\{\cos^2\left[\phi + \tan^{-1}\frac{T}{\pi}\frac{\dot{m}_0(-\tau)}{m_0(-\tau)}\right]\right\}^\alpha \right. \\ \left. + \left\{\cos^2\left[\phi - \tan^{-1}\frac{T}{\pi}\frac{\dot{m}_0(-\tau)}{m_0(-\tau)}\right]\right\}^\alpha\right\}.\end{aligned} \tag{85}$$

Averaging with respect to ϕ and τ yields

$$\Pr[\text{error}] = \frac{\beta C_\alpha}{2}\left[\frac{\mathcal{E}_0}{E_2}\right]^\alpha \int_{-\infty}^{\infty}\left\{\left[\frac{T}{\pi}\,\dot{m}_0(-\tau)\right]^2 + [m_0(-\tau)]^2\right\}^\alpha d\tau. \tag{86}$$

It can be shown that, for the frequency shift keyed signal $s_c(t)$, the average power on the channel is

$$\bar{W} = E^2[(1/4A_0^2) + \tfrac{1}{2}I_1], \tag{87}$$

where

$$A_0 = |H(\pm\omega_s)| = |H(\pm\omega_m)|. \tag{88}$$

The first term in the bracket of (87) is the result of discrete components of the signal at the mark and space frequencies. Substituting (87) into (86) and rearranging some of the terms yields

$$\begin{aligned}\Pr[\text{error}] = \frac{\beta C_\alpha T}{2}\left[\frac{\mathcal{E}_0\left(\dfrac{1}{2A_0^2} + I_1\right)}{2\bar{W}T}\right]^\alpha \\ \cdot\int_{-\infty}^{\infty}\left\{T\left[\frac{T}{\pi}\,\dot{m}_0(t)\right]^2 + T[m_0(t)]^2\right\}^\alpha \frac{dt}{T}\end{aligned} \tag{89}$$

where $\bar{W}T/\mathcal{E}_0$ is the signal-to-noise ratio defined previously.

In the same manner as for the systems considered previously, an equivalent receiving filter characteristic $H(\omega)$ is to be found which minimizes the error rate when α is equal to 1. For that value of α, the probability of error is equal to

$$\begin{aligned}\Pr[\text{error}] = \frac{\beta T}{8}\left[\frac{\mathcal{E}_0}{\bar{W}T}\right]\left[\frac{1}{2A_0^2} + \frac{1}{2\pi T}\int_{-\infty}^{\infty}\left|\frac{Y_0(\omega)}{H(\omega)}\right|^2 d\omega\right] \\ \cdot\int_{-\infty}^{\infty}\left[\frac{T^2}{\pi^2}\,\dot{m}_0^2(t) + m_0^2(t)\right]dt,\end{aligned} \tag{90}$$

where

$$\frac{1}{A_0^2} = \frac{1}{2}\int_{-\infty}^{\infty}\left[\delta\left(\omega - \frac{\pi}{T}\right) + \delta\left(\omega + \frac{\pi}{T}\right)\right]\left|\frac{1}{H(\omega)}\right|^2 d\omega. \tag{91}$$

By Parseval's theorem

$$\int_{-\infty}^{\infty} \dot{m}_0^2(t)\ dt = \frac{1}{2\pi} \int_{-\infty}^{\infty} \omega^2 \mid M_0(\omega) \mid^2 d\omega.$$

Therefore, for a value of α equal to 1, (90) may be rewritten

$$\begin{aligned} \Pr[\text{error}] = \frac{\beta}{(4\pi)^2} \left[\frac{\varepsilon_0}{\bar{W}T}\right] \int_{-\infty}^{\infty} \left\{ \frac{\pi T}{2} \left[\delta\left(\omega - \frac{\pi}{T}\right) + \delta\left(\omega + \frac{\pi}{T}\right) \right] \right. \\ \left. + \mid Y_0(\omega) \mid^2 \right\} \left| \frac{1}{H(\omega)} \right|^2 d\omega \cdot \int_{-\infty}^{\infty} \left(\frac{T^2}{\pi^2} \omega^2 + 1 \right) \mid N_0(\omega) H(\omega) \mid^2 d\omega. \end{aligned} \quad (92)$$

For ease of notation, let

$$\begin{aligned} a(\omega) &\triangleq \pi T/2\{\delta[\omega - (\pi/T)] + \delta[\omega + (\pi/T)]\} + \mid Y_0(\omega) \mid^2 \\ b(\omega) &\triangleq [(T^2/\pi^2)\omega^2 + 1] \mid N_0(\omega) \mid^2 \\ h(\omega) &\triangleq \mid H(\omega) \mid^2. \end{aligned} \quad (93)$$

To minimize the probability of error, it is necessary to find the function $h(\omega)$ which minimizes the product.

$$P = \int_{-\infty}^{\infty} \frac{a(\omega)}{h(\omega)}\, d\omega \int_{-\infty}^{\infty} b(\omega) h(\omega)\ d\omega. \quad (94)$$

The minimum occurs when the variation

$$\begin{aligned} \delta P = \int_{-\infty}^{\infty} \frac{a(\omega)}{h(\omega)}\, d\omega \int_{-\infty}^{\infty} b(\omega)\, \delta h(\omega)\ d\omega \\ - \int_{-\infty}^{\infty} \frac{a(\omega)}{h^2(\omega)}\, \delta h(\omega_2)\ d\omega \int_{-\infty}^{\infty} b(\omega) h(\omega)\ d\omega \end{aligned} \quad (95)$$

$$\delta P = \int_{-\infty}^{\infty}\int_{-\infty}^{\infty} \left[\frac{a(\omega_1)}{h(\omega_1)}\, b(\omega_2) - \frac{a(\omega_2)}{h^2(\omega_2)}\, b(\omega_1) h(\omega_1) \right] \delta h(\omega_2)\ d\omega_1\, d\omega_2$$

is equal to zero. Since it must be equal to zero for any variation $\delta h(\omega_2)$, the bracketed term must be zero

$$\frac{a(\omega_1)}{h(\omega_1)}\, b(\omega_2) - \frac{a(\omega_2)}{h^2(\omega_2)}\, b(\omega_1) h(\omega_1) = 0 \quad (96)$$

for all values of ω_1 and ω_2. This requires that $h^2(\omega)b(\omega)/a(\omega)$ be equal to a constant. It can be shown that the second variation $\delta^2 P$ is positive when the above condition is met, so that P is truly at a minimum, and not at a maximum or stationary point. To minimize the probability of error, the filter characteristic must satisfy

$$| H(\omega) |^2 \sim \left\{ \frac{\frac{\pi T}{2} \left[\delta\left(\omega - \frac{\pi}{T}\right) + \delta\left(\omega + \frac{\pi}{T}\right) \right] + | Y_0(\omega) |^2}{\left(\frac{T^2}{\pi^2} \omega^2 + 1\right) | N_0(\omega) |^2} \right\}^{\frac{1}{2}}. \tag{97}$$

The impulses in the receiving filter characteristics correspond to suppression of the discrete components at the transmitting filter. Since it is not feasible to construct such a filter, it is assumed that the suboptimum "smooth" filter, given by

$$| H(\omega) |^2 \sim \frac{| Y_0(\omega) |}{\left(\frac{T^2}{\pi^2} \omega^2 + 1\right)^{\frac{1}{2}} | N_0(\omega) |} \tag{98}$$

is to be used.

The conditional error rate, defined as the average number of bit errors per noise burst, is given by

$$\begin{aligned} \bar{N} = \frac{C_\alpha}{2} \left[\frac{\varepsilon_0}{\bar{W} T} \right]^\alpha \left[\frac{1}{4A_0} + \frac{1}{2} I_1 \right]^\alpha \\ \cdot \int_{-\infty}^{\infty} \left\{ T \left[\frac{T}{\pi} \dot{m}_0(t) \right]^2 + T[m_0(t)]^2 \right\}^\alpha \frac{dt}{T}. \end{aligned} \tag{99}$$

The general expression for $\bar{N}$ is evaluated for the same special case described previously. The spectrum of an individual data pulse is the raised cosine spectrum, and the spectrum of the noise is assumed to be constant in the band of interest. The expression for $\bar{N}$ has been numerically evaluated, on a digital computer, for values of α equal to 1, 2, and 3. The results are tabulated below, and are plotted in Fig. 12.

α	$\bar{N}$
1	$0.402\ \varepsilon_0/\bar{W}T$
2	$0.392\ (\varepsilon_0/\bar{W}T)^2$
3	$0.48\ (\varepsilon_0/\bar{W}T)^3$

V. PHASE SHIFT KEYING SYSTEM WITH DIFFERENTIALLY COHERENT DETECTION

5.1 *Binary (Two Phase) System*

The ideal data receiver utilizing differentially coherent detection consists of a receiving filter $H_c(\omega)$ symmetrical about the carrier frequency ω_c, followed by a detector. The differentially coherent detector multi-

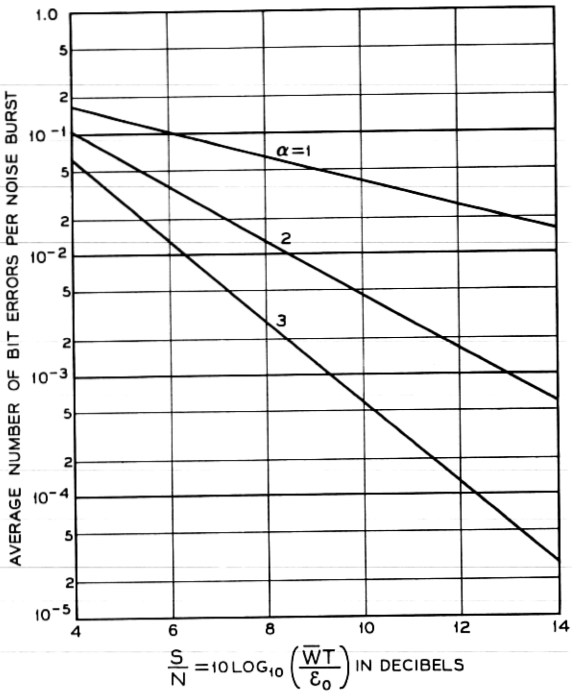

Fig. 12 — Performance of frequency shift keyed system.

plies the received signal by the signal which had been received one bit duration earlier. The output of the detector is applied to a synchronous decision device of the type described previously, in the analysis of the double-sideband AM system. A block diagram of the receiver is shown below, in Fig. 13.

In the absence of noise, the signal at the input to the detector is of the form

$$s_r(t) = y(t) \cos \omega_c t \tag{100}$$

where the modulating signal $y(t)$ satisfies (6) The multiplier a_i may be ± 1. If the ith bit is a mark, a_i is made equal to a_{i-1} ; if a space, a_i equal to $-a_{i-1}$. In the absence of noise, the signal at the output of the detector is equal to

$$v_0(t) = y(t)y(t - T) \cos \omega_c(t) \cos \omega_c(t - T). \tag{101}$$

The carrier frequency ω_c is selected to be an integral multiple of the bit

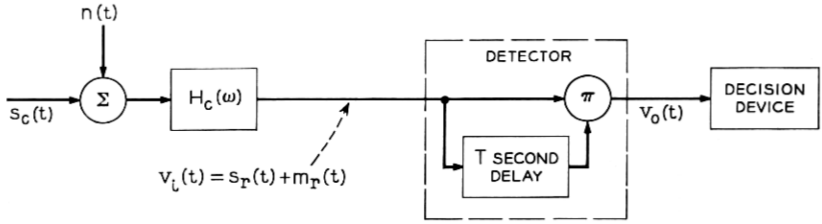

Fig. 13 — Receiver for binary phase shift keyed system with differentially coherent detection.

rate, so that $\omega_c T$ is an integral multiple of 2π. At the ith sampling instant, the signal at the output of the detector is equal to

$$v_0(iT) = y(iT)y[(i-1)T] = a_i a_{i-1} E^2. \tag{102}$$

The sample is equal to $+E^2$ if the ith bit is a mark, and $-E^2$ if it is a space. The decision device produces a mark symbol if the sample is positive and a space symbol if it is negative.

Let $t = 0$ denote the sampling instant for an arbitrarily chosen data pulse, and let $t = \tau$ denote the time of occurrence of the closest noise burst. At the sampling instant $t = 0$, the output of the detector is

$$v_0(0) = [a_0 E + K m_0(-\tau) \cos \psi][a_{-1} E + K m_0(-\tau - T) \cos \psi]. \tag{103}$$

To find the probability of error, given τ and ψ, it is necessary to find the ranges of values of K which cause the polarity of $v_0(0)$ to be reversed. For ease of notation, let the following two functions of τ and ψ be defined:

$$\begin{aligned} B_1(\tau,\psi) &\triangleq \frac{E}{m_0(-\tau) \cos \psi} \\ B_2(\tau,\psi) &\triangleq \frac{E}{m_0(-\tau - T) \cos \psi}. \end{aligned} \tag{104}$$

The output of the detector, at the sampling instant $t = 0$, may be written

$$v_0(0) = E^2[a_0 + (K/B_1)][a_{-1} + (K/B_2)]. \tag{105}$$

Depending on the values of τ and ψ, B_1 and B_2 may each be either positive or negative, so that there are four possible combinations of polarity. In addition, either B_1 or B_2 may have the larger absolute value. Each of these eight possible combinations of polarity and relative absolute value must be investigated separately. The range of K which causes a reversal of polarity, depending on the values of a_0 and a_{-1}, is to be found. This is most clearly done graphically. In Fig. 14, the eight possible combina-

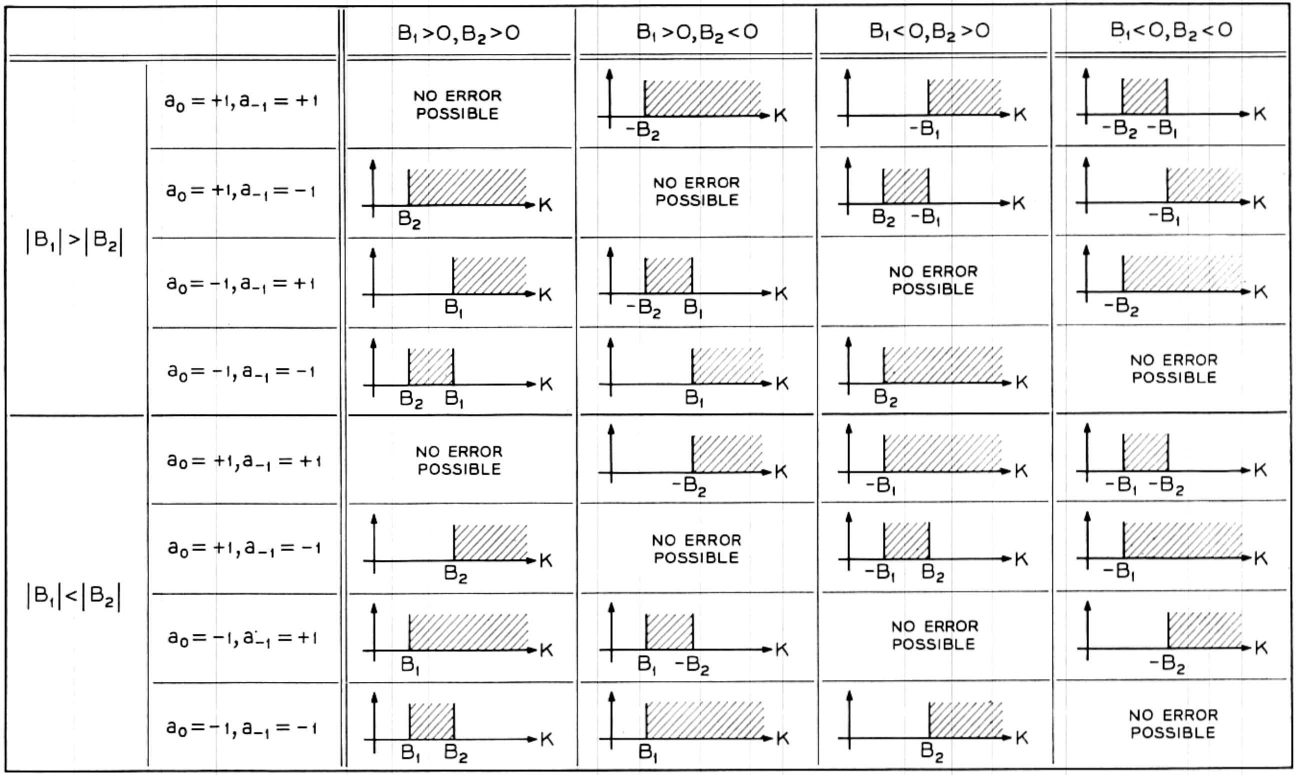

Fig. 14 — Error regions for the noise burst amplitude.

tions are shown separately and, for each of the four equally probable combinations of a_0 and a_{-1}, the range of K which causes an error is shown shaded. Because the four combinations of a_0 and a_{-1} are equally probable, each with probability of occurrence equal to $\frac{1}{4}$, the probability of error, given τ and ψ, for any one of the eight possibilities for B_1 and B_2, is equal to

$$\Pr[\text{error} \mid \tau,\psi] = \tfrac{1}{4} \sum_{a_0,a_{-1}} \Pr[K \text{ in shaded region}]. \tag{106}$$

It may be seen in Fig. 14 that, for each of the eight possibilities, this is equal to

$$\Pr[\text{error} \mid \tau,\psi] = \tfrac{1}{2} \Pr[K > \min (\mid B_1 \mid, \mid B_2 \mid) \mid \tau,\psi] \tag{107}$$

The probability of error, given τ and ψ, may be rewritten,

$$\Pr[\text{error} \mid \tau,\psi] = \tfrac{1}{2} \Pr\left\{ \varepsilon > \frac{E^2}{\cos^2 \psi \max [m_0^2(-\tau), m_0^2(-\tau - T)]} \,\middle|\, \tau,\psi \right\} \tag{108}$$

and, by (5) this is equal to

$$\Pr[\text{error} \mid \tau,\psi] = \frac{1}{2} \left\{ \frac{\varepsilon_0 \cos^2 \psi \max [m_0^2(-\tau), m_0^2(-\tau - T)]}{E^2} \right\}^{\alpha}. \tag{109}$$

Averaging with respect to ψ and τ yields

$$\Pr[\text{error}] = \frac{\beta C_\alpha}{2} \left[\frac{\varepsilon_0}{E^2} \right]^{\alpha} \int_{-\infty}^{\infty} \{\max [m_0^2(-\tau), m_0^2(-\tau - T)]\}^{\alpha} \, d\tau. \tag{110}$$

The signal on the channel $s_c(t)$ is the same as that for the double-sideband AM system. The average transmitted power is therefore given by (21). Substituting this into (110), dividing by βT, and rearranging terms, yields that the conditional error rate is equal to

$$\bar{N} = \frac{C_\alpha}{2} \left[\frac{1}{2} I_1 \frac{\varepsilon_0}{\bar{W}T} \right]^{\alpha} \int_{-\infty}^{\infty} \{\max [Tm_0^2(t), Tm_0^2(t - T)]\}^{\alpha} \frac{dt}{T} \tag{111}$$

where $\bar{W}T/\varepsilon_0$ is the signal-to-noise ratio as defined previously.

In order to obtain numerical results, the general expression for $\bar{N}$ given above is evaluated for the same special case as the preceding systems. The spectrum of a single data pulse is the raised cosine spectrum, and the spectrum of the noise burst is assumed to be constant in the band of interest. The equivalent receiving filter characteristic $H(\omega)$ is the same as that for the AM systems. The expression for $\bar{N}$ has been numerically evaluated, on a digital computer, for values of α equal to 1, 2, and 3. The results are tabulated below, and are plotted in Fig. 15.

α	$\bar{N}$
1	$0.236\ (\mathcal{E}_0/\bar{W}T)$
2	$0.109\ (\mathcal{E}_0/\bar{W}T)^2$
3	$0.0625\ (\mathcal{E}_0/\bar{W}T)^3$

5.2 *Quaternary (Four Phase) System*

A quaternary phase shift keying system transmits a signal which, at the discrete sampling instants, may have any one of four possible phases spaced 90° apart. Such a signal is mathematically equivalent to two binary signals in quadrature, where each binary signal is of the form described in the preceding section.

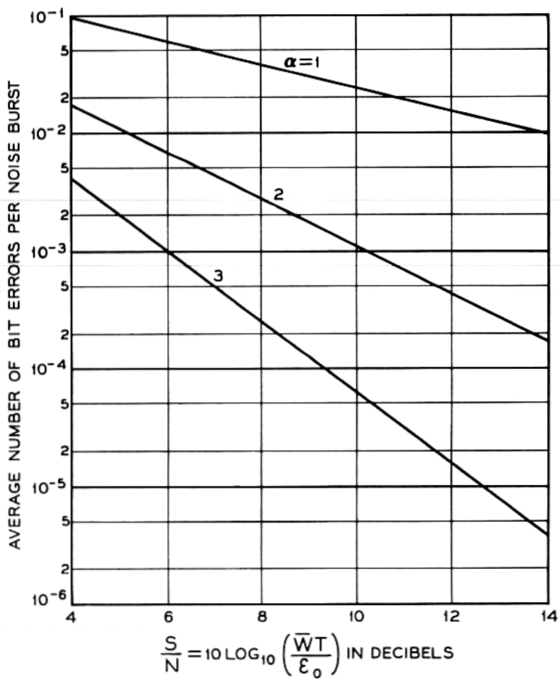

Fig. 15 — Performance of binary phase shift keyed system with differentially coherent detection.

The transmitted signal consists of an "in-phase" binary signal and "quadrature" binary signal. The ideal data receiver consists of a receiving filter $H_c(\omega)$, centered about the carrier frequency ω_c, followed by two separate binary receivers. One of these, identical to the receiver of the preceding section, is sensitive to the "in-phase" binary signal. The other binary receiver, preceded by a phase shifting network with a phase characteristic which is equal to $-\pi/2$ radians throughout the frequency band of the received signal, is sensitive to the "quadrature" binary signal. A block diagram of the receiver is shown in Fig. 16. The system operates in the following manner. In the absence of noise, the signal at the output of the receiving filter is of the form

$$s_r(t) = y_a(t) \cos \omega_c t - y_b(t) \sin \omega_c t, \tag{112}$$

where the modulating signals are each of the form given by (6). At the sampling instants the second term of (112) is equal to zero, and the "a" system is identical to the binary system described in the preceding section. In the absence of noise, the signal at the input to the "b" detector is given by the Hilbert transform

$$\hat{s}(t) = y_b \cos \omega_c t + y_a \sin \omega_c t. \tag{113}$$

At the sampling instants the second term of (113) is equal to zero, and the "b" system is also identical to the binary system. At any arbitrarily chosen sampling instant Pr["a" bit in error] and Pr["b" bit in error] are both given by (110). The average number of bits in error per symbol transmitted is equal to

$$\begin{aligned} \bar{P} = \Pr[\text{“}a\text{” bit in error, “}b\text{” bit correct}] \\ + \Pr[\text{“}b\text{” bit in error, “}a\text{” bit correct}] \\ + 2\Pr[\text{“}a\text{” bit and “}b\text{” bit both in error}]. \end{aligned} \tag{114}$$

The Venn diagram in Fig. 17 shows that this is equal to

$$\bar{P} = \Pr[\text{“}a\text{” bit in error}] + \Pr[\text{“}b\text{” bit in error}]. \tag{115}$$

The average number of bits in error per symbol transmitted is therefore,

$$\bar{P} = \beta C_\alpha \left[\frac{\varepsilon_0}{E^2}\right]^\alpha \int_{-\infty}^{\infty} \{\max [m_0^2(-\tau), m_0^2(-\tau - T)]\}^\alpha \, d\tau. \tag{116}$$

Since there are, on the average, βT noise bursts per symbol transmitted, the average number of bits in error per noise burst is equal to

$$\bar{N} = \bar{P}/\beta T. \tag{117}$$

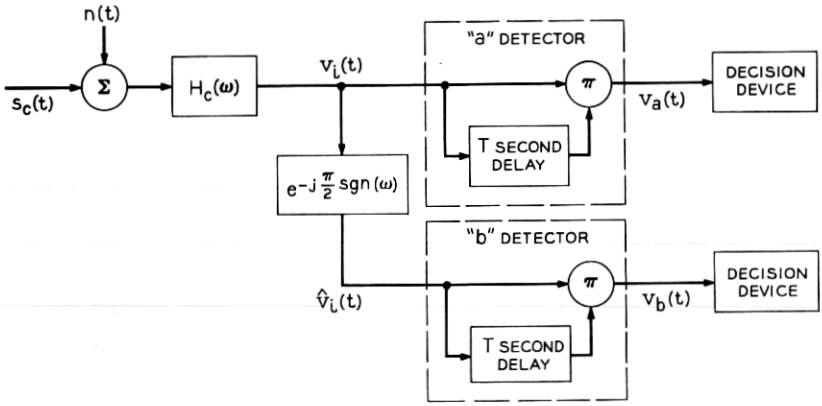

Fig. 16 — Receiver for quaternary phase shift keyed system with differentially coherent detection.

The transmitted signal consists of two binary signals in quadrature. Since the two binary signals are orthogonal, the average power of the transmitted signal is equal to the sum of the average powers of the two binary signals, and is twice the power for the binary system. Substituting this and (117), into (116) and rearranging terms yields

$$\bar{N} = C_\alpha \left[I_1 \frac{\varepsilon_0}{\bar{W}T} \right]^\alpha \int_{-\infty}^{\infty} \{\max\,[Tm_0^2(t), Tm_0^2(t-T)]\}^\alpha \frac{dt}{T}, \quad (118)$$

where in this case, $\bar{W}T/2\varepsilon_0$ is the signal-to-noise ratio, described previously as the signal energy per bit divided by the minimum energy per noise burst. When $\bar{N}$ is plotted versus $10 \log_{10} [\bar{W}T/2\varepsilon_0]$ db as the abscissa, the value is twice that for the binary case.

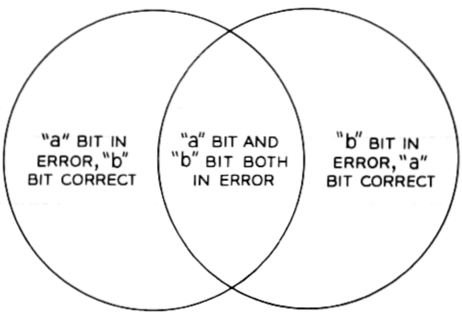

Fig. 17 — Venn diagram for decision outcomes.

VI. COMPARISON OF THE MODULATION SYSTEMS

In the preceding three sections, the various data transmission systems have been analyzed, and the performance of each in the presence of impulsive noise has been determined. It is of interest to compare these results and to rank the systems as to performance. For each of the modulation systems, an expression has been derived for the average number of bit errors per noise burst, as a function of the signal-to-noise ratio. The systems may be ranked by comparing the signal-to-noise ratios required by the different systems for the same error rate.

Such a comparison is done here for the special case for which $\bar{N}$ has been evaluated. The spectrum of an individual data pulse is the raised cosine spectrum, and the spectrum of the noise burst is assumed to be constant in the band of interest. The equivalent receiving filter for each system is the one which minimizes $\bar{N}$ when α is equal to 1. (In those cases for which the optimum filter has impulses in its response, corresponding to carrier suppression at the transmitter, the suboptimum "smooth" filter is assumed. This is described in the preceding sections.)

For each of the modulation systems, the average number of bit errors per noise burst is given by the expression

$$\bar{N} = \left[C \frac{\mathcal{E}_0}{\bar{W}T} \right]^\alpha, \tag{119}$$

where the constant C depends on the type of modulation system, the characteristics of the receiving filter, and the value of α. The systems may be ranked by comparing the values of C. The ratio between the values of C for any two systems is the difference in signal-to-noise ratio required for equal error rate. In Fig. 18, the values of C for the various modulation systems are plotted as functions of α.

The comparison of Fig. 18 shows the modulation systems to be ranked in the following order:

(1.) Single-sideband AM with coherent detection.
(2.) Double-sideband AM with coherent detection.
(3.) Phase shift keying with differentially coherent detection.
(4.) Frequency shift keying.
(5.) AM with envelope detection.

It is interesting to note that this is the same ranking as has been determined for performance in the presence of Gaussian noise.

VII. COMPLEMENTARY DELAY FILTERS

In the sections on the performances of the various modulation systems, the general expressions for the error rate have been evaluated for

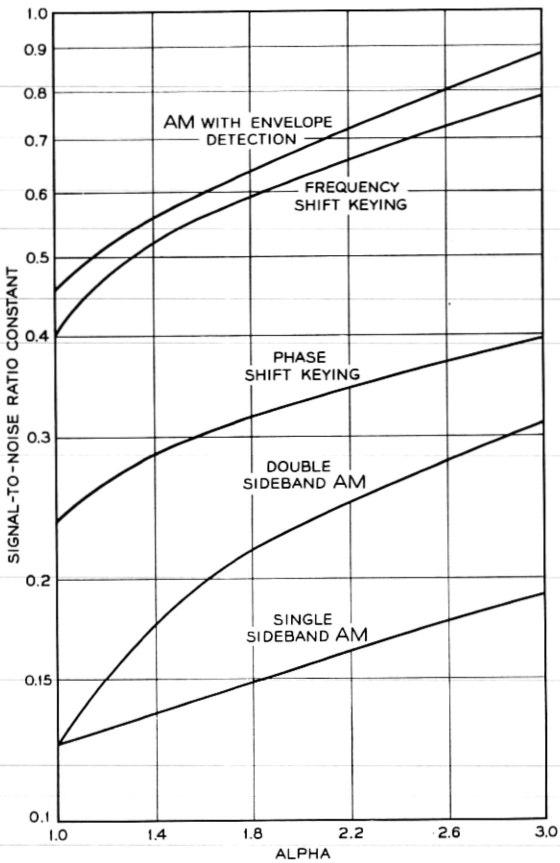

Fig. 18 — Comparison of modulation systems.

a special case which is of wide interest. For the purpose of those evaluations, the equivalent receiving filter $H(\omega)$ has been given an amplitude characteristic $A(\omega)$ which minimizes the error rate for the worst case, when α is equal to 1, and a phase characteristic $\phi(\omega)$ which is zero or a linear function of frequency

$$\phi(\omega) = -D\omega. \tag{120}$$

Such a phase characteristic causes a pure delay of D seconds, with no distortion. Since this corresponds merely to shift of the time axis, and affects signal and noise identically, it has no effect. It has been pointed out previously that, for values of α greater than 1, a phase characteristic

$\phi(\omega)$ which is a function of frequency other than linear can serve to reduce the error rate. This effect is now discussed.

When the phase characteristic is other than a linear function, the envelope delay

$$D(\omega) = -\frac{d}{d\omega}\phi(\omega) \tag{121}$$

is not constant, but varies with frequency. When the noise burst passes through such a filter, its various frequency components are delayed by different amounts, and its energy is spread out over many bits. The peak value of the spread out burst is much lower than the peak value of the original burst, so that many bursts which would have caused errors no longer do so.

In the analyses of the systems, the individual data pulses at the receiving filter output are each constrained to be a specific function $y_0(t)$. This implies that at the transmitter the data pulses pass through a transmitting delay filter, with envelope delay equal to

$$D_T(\omega) = D - D(\omega)$$

in the frequency band of the data signal. The constant D, at least as large as the maximum value of $D(\omega)$, is necessitated by the fact that, for realizability, $D_T(\omega)$ must be positive. The two delay filters exactly complement one another, so that the net effect on the data signal is a pure delay, with no distortion. The noise burst, occurring on the channel after the transmitting filter, only passes through the second filter and is spread out.

The use of such complementary delay filters, based on heuristic reasoning of the type given above, has been suggested previously.[4,11] In this section, the improvement which results from the use of such filters, in terms of the equivalent increase in signal-to-noise ratio which would be required for an equal reduction in error rate, is presented.

Three types of delay networks, which lend themselves to synthesis, have been considered. One of these, called a "linear delay network," has an envelope delay characteristic given by

$$D_1(\omega) = (D_m T/2\pi)\omega \operatorname{sgn}(\omega) \quad \text{for} \quad |\omega| < 2\pi/T \tag{122}$$

and hence a phase characteristic equal to

$$\phi_1(\omega) = -(D_m T/4\pi)\omega^2 \operatorname{sgn}(\omega) \quad \text{for} \quad |\omega| < 2\pi/T, \tag{123}$$

where D_m is the maximum delay in the band of interest. The other two types are called "sinusoidal delay networks." One of these, with a half cycle of sinusoid in the band of interest has an envelope delay characteristic

$$D_2(\omega) = D_m \cos \omega T/4 \quad \text{for} \quad |\omega| < 2\pi/T \tag{124}$$

and hence a phase characteristic equal to

$$\phi_2(\omega) = -(4D_m/T) \sin \omega T/4 \quad \text{for} \quad |\omega| < 2\pi/T. \tag{125}$$

The third type is a sinusoidal delay network with a full cycle of sinusoid in the band of interest. It has an envelope delay characteristic given by

$$D_3(\omega) = (D_m/2)[1 + \cos \omega T/2] \quad \text{for} \quad |\omega| < 2\pi/T \tag{126}$$

and hence a phase characteristic

$$\phi_3(\omega) = (D_m/T)[(\omega T/2) + \sin \omega T/2] \quad \text{for} \quad |\omega| < 2\pi/T. \tag{127}$$

The three envelope delay chacteristics are shown in Fig. 19.

The general expressions for the error rate, derived previously for the various modulation systems, have been evaluated on a digital computer, with the equivalent receiving filter having each of the above phase characteristics. Values of maximum delay up to 10 symbol durations have been considered. The resulting error rates are compared with those

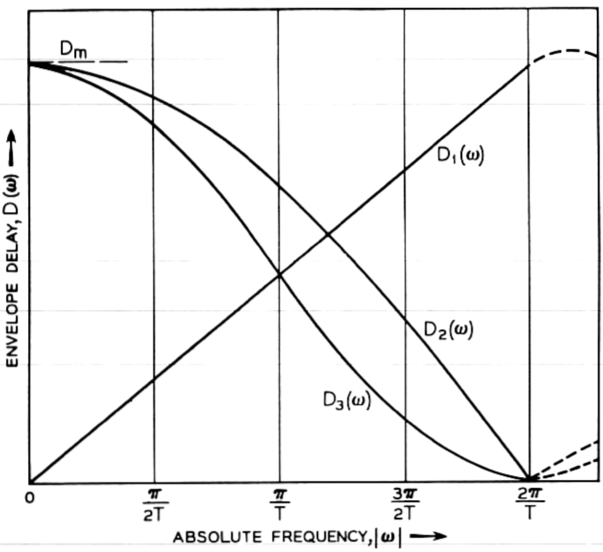

Fig. 19 — Envelope delay characteristics.

when no delay is included, and the improvement is plotted, as a function of the maximum delay, in Figs. 20 through 23.

For all but the differentially coherent phase shift keying systems, the delay networks have no effect for a value of α equal to 1. This has been discussed in the preceding sections; by Parseval's theorem the phase characteristics of the noise have no effect when α is equal to 1. As the value of α increases, the networks become more effective. This phenomenon is to be expected. When the noise burst is spread over many bits, the peak value is reduced and many bursts which would have caused errors no longer do so. However, this improvement is reduced somewhat by the fact that bursts of very large amplitude remain large enough, even after spreading, to cause errors. Such bursts, which would have caused one or two errors, now cause many. As α increases, the percentage of such high amplitude bursts decreases, and the improvement increases. This effect, which reduces the over-all improvement to be gained by the use of complementary delay filters, prompts the consideration of limiting at the input to the delay filter at the receiver. If the limiter is set to a value just above the peak value of the signal, bursts of very high amplitude are clipped and after spreading, will not cause as many errors as they would have without limiting.

A precise analysis of the effect of limiting prior to spreading is not practicable. The process is nonlinear, and the response of the combined limiter-filter depends strongly on the amplitude K and time of occurrence

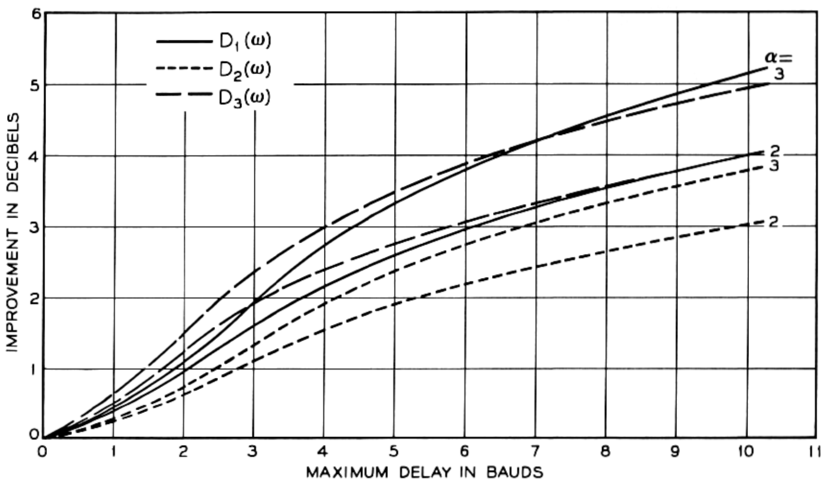

Fig. 20 — Effect of complementary delay networks on double sideband AM systems.

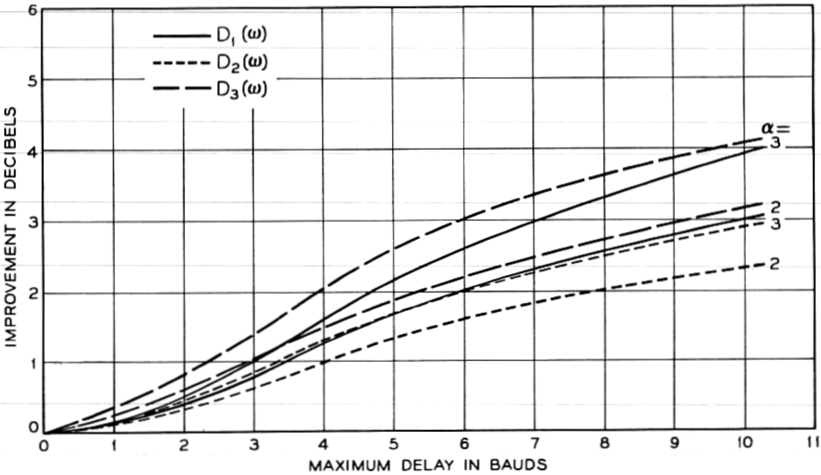

Fig. 21 — Effect of complementary delay networks on single-sideband AM system.

τ of the noise burst, as well as on the particular data sequence being transmitted. In addition, the results of such an analysis would be quite sensitive to the model chosen to represent the channel. In the systems discussed in this paper, the transmission medium and receiving filter have both been linear, and it was therefore possible to combine their

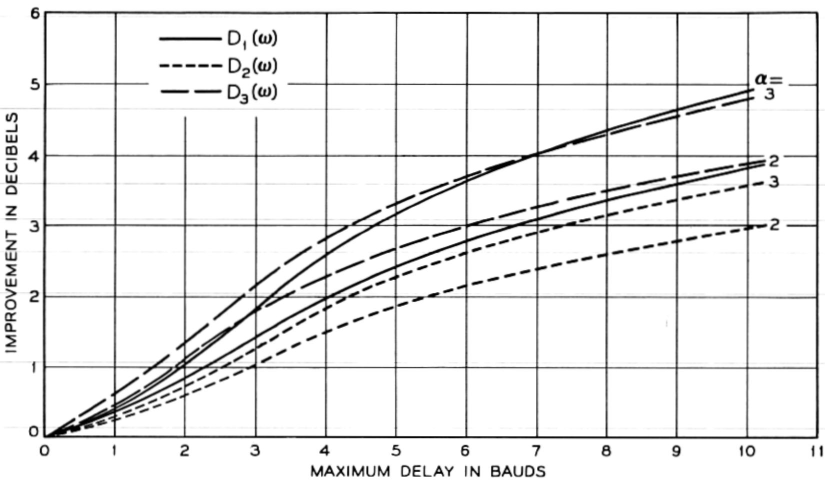

Fig. 22 — Effect of complementary delay networks on frequency shift keyed system.

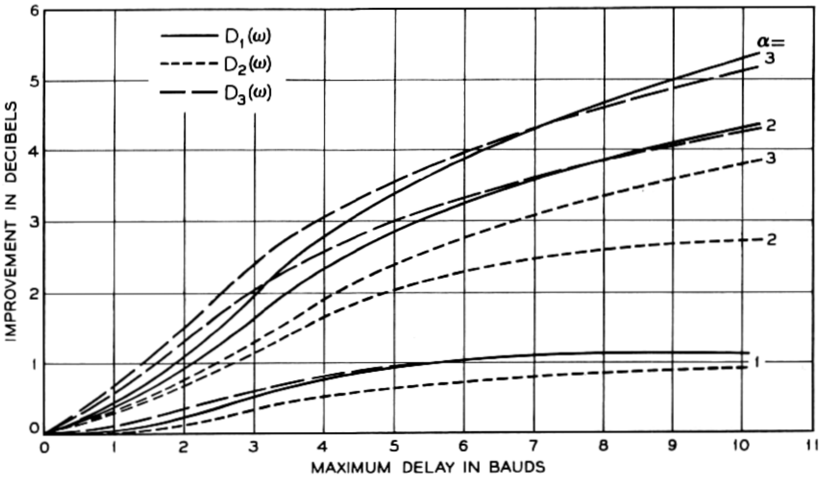

Fig. 23 — Effect of complementary delay networks on differentially coherent phase shift keyed system.

characteristics for the purpose of analysis. The channel was considered to have unity gain in the band of frequencies passed by the receiver band-pass filter; the transmission characteristics of the channel at frequencies outside that band had no effect on the signal or noise at the output of the filter. If limiting is introduced, however, it is most effective if it is done at the point where the noise bursts are most impulsive. This point is at the input to the receiver, prior to any filtering or spreading, where their spectrum is widest. With a nonlinear device between the channel and the receiving filter, their characteristics cannot be combined. The effect of the limiting depends very much on the transmission characteristics of the channel outside the pass band of the filter. If the channel has a considerably wider band than the filter, the limiting will be much more effective than if the bandwidths are comparable.

For these reasons, an analytic evaluation of the improvement resulting from the introduction of limiting is not practicable. An evaluation by simulation techniques or experimental procedures is more feasible. Limiting is discussed in this paper only to point out that further improvement is possible.

VIII. ACKNOWLEDGMENT

This article is taken from the author's Ph.D. dissertation at the Polytechnic Institute of Brooklyn. Thanks are due Prof. M. Schwartz for his assistance as thesis advisor.

The author is particularly indebted to J. Salz, M. A. Rappeport, and A. P. Stamboulis of the Bell Telephone Laboratories. Their comments and assistance have been invaluable.

REFERENCES

1. Alexander, A. A., Gryb, R. M., and Nast, D. W., Capabilities of the Telephone Network for Data Transmission, B.S.T.J., *39*, May, 1960, pp. 431–476.
2. Berger, J. M. and Mandelbrot, B., A New Model for Error Clustering in Telephone Circuits, I.B.M. J. Research and Development, July, 1963.
3. Fennick, J. H., A Report on Some Characteristics of Impulse Noise in Telephone Communication Systems, Conference Paper 63–986, I.E.E.E., June, 1963.
4. Knox-Seith, J., Pulse Transmission, Patent No. 3032725, May 1, 1962.
5. Mertz, P., Model of Impulsive Noise for Data Transmission, I.R.E. Trans. Communications Systems, June, 1961.
6. Mertz, P., Statistics of Hyperbolic Error Distributions in Data Transmission, I.R.E. Trans. Communications Systems, December, 1961.
7. Morris, R., Further Analysis of Errors in Capabilities of the Telephone Network for Data Transmission, B.S.T.J., *41*, July, 1962, pp. 1399–1414.
8. Nyquist, H., Certain Topics in Telegraph Transmission Theory, Trans. A.I.E.E., April, 1928.
9. Sunde, E. D., Ideal Binary Pulse Transmission by AM and FM, B.S.T.J., *38*, Nov., 1959. pp. 1357–1426.
10. Sussman, S. M., Analysis of the Pareto Model for Error Statistics on Telephone Circuits, I.E.E.E. Trans. Communications Systems, June, 1963.
11. Wainwright, R. A., On the Potential Advantage of a Smearing-Desmearing Filter Technique in Overcoming Impulse-Noise Problems in Data Systems, I.R.E. Trans. Communications Systems, December, 1961.